FINITE ELEMENT MODELING OF GEOSYNTHETIC REINFORCED PAVEMENT SUBGRADES

By

ABDELAZIZ AHMED BOHAGR

A thesis submitted in partial fulfillment of
the requirements for the degree of

MASTER OF SCIENCE IN CIVIL ENGINEERING

WASHINGTON STATE UNIVERSITY

Department of Civil and Environmental Engineering

July 2013

To the Faculty of Washington State University:

The members of the Committee appointed to examine the thesis of ABDELAZIZ AHMED BOHAGR find it satisfactory and recommend that is be accepted.

Balasingam Muhunthan, Ph.D, Chair

William Cofer, Ph.D.

Haifang Wen, Ph.D.

ACKNOWLEDGEMENT

First and foremost, I would like to express my gratitude to my advisor, Dr. Balasingam Muhunthan. Dr. Muhunthan has guided me in several aspects of my development as a graduate student, not only by giving me the opportunity to pursue exciting and relevant research but also by teaching me to present my work in a precise and elegant manner. His invaluable knowledge, patience and continuous support made every second of the project immensely gratifying. His dedication and love for research and academic excellence have rubbed off on me. More of all, he has been a friend and a mentor whenever I needed one.

I would like to express my sincere gratitude to my committee members, Dr. William Cofer and, Dr. Haifang Wen for helping me expand my knowledge about various aspects in my field and this paper, too. In addition, special thanks to the staff of Civil Engineering Department.

I would like to thank the Libyan government for giving me this precious opportunity to pursue my Master degree from a very highly respected university.

Most importantly, special dedication to my father's soul whose unselfish, compassionate, and loyal spirit guided me all the time and my dear mother who helped me achieve this paper. Finally, my special thanks to my brothers, my sisters and my fiancée.

FINITE ELEMENT MODELING OF GEOSYNTHETIC REINFORCED

PAVEMENT SUBGRADES

Abstract

By Abdelaziz Ahmed Bohagr, M. S.
Washington State University
July 2013

Chair: Balasingam Muhunthan

Use of a geosynthetic as a reinforcement material in the base course layer of flexible pavement has been shown to improve the performance of flexible pavements including increased pavement service life, reduction in base course thickness, rut depth, fatigue strain, and reflective cracking. Various finite element models have been used to simulate the behavior of pavement layers under different types of loading conditions. Many of these approaches have concentrated on the prediction of the contribution of geosynthetics fibers to increased shear strength.

In this study, finite element analyses are conducted using ADINA on pavement cross-sections to investigate the effects of the base layer and subgrade layer quality on the performance of reinforced pavements under monotonic loading, as well as to study the effects of the interface friction between the geosynthetics and pavement layers (base and subgrade) on the performance of flexible pavements.

The distribution of the vertical surface deflection, the horizontal displacement, and the volumetric strain under monotonic loadings for the various cases of base courses and interface friction were studied. The results show that the vertical surface deflection and the horizontal displacement improved when the interface friction between the geosynthetics and the pavement layers increased. The amount of improvement, however, was dependent on the quality of the base and the subgrade layers.

TABLE OF CONTENTS

LIST OF TABLES

LIST OF FIGURES

CHAPTER ONE

INTRODUCTION

1.1 Introduction

Geotextiles and geomembranes have been widely used over the last few decades in many engineering applications. Most of these materials are constituted of synthetic fibers, and each has different properties and applications.

Geotextiles are permeable fibers, often used as reinforcement materials to enhance soil properties such as shear strength. They are used for civil engineering applications such as roads, airfield rail roads, retaining structures, reservoirs, canals and dams. Geotextiles are classified into two categories based on their production; Woven or non-woven. Woven geotextiles have a visible distinct construction pattern. They are often used for load distribution, soil separation, filtration, reinforcement and drainage. Non-woven Geotextiles have a random pattern without any visible pattern. They are often used for load distribution, soil separation and stabilization, but rarely used for soil reinforcement such as retaining walls.

The main purpose of geomembranes is to control the movement of liquid. It is commonly used in landfills to help to prevent chemicals and other dangerous leachates from polluting the surrounded area. It is also used to line canals, pits and ponds.

Many researchers have studied the effect of geosynthetics when used as reinforcement materials in soil applications. Rowe et al. (2001) investigated the short-term behavior of a reinforced soil wall constructed on a yielding foundation and analyzed the key factors influencing the wall behavior. In their study, they used the finite element method to calculate the

deformation response and compared it with observed behavior. It was found that the analysis gave the best results when the interface friction angle between the backfill and wall facing was between (30^0 – 45^0). They also found that the stiffness and the strength of the foundation had a significant effect on wall behavior when geosynthetics was used as reinforcement materials.

Various finite element models have been used to simulate and describe the behavior of pavement layers under different types of loading conditions. Many of the modeling approaches that were developed have concentrated on the prediction of the contribution of geo-fibers to increase in shear strength. The techniques that were used to describe the shear strength increase were based on force equilibrium, energy dissipation, the superposition of the sand and fiber effects, and friction and interlocking (Diambra et al. 2010).

The response of geotextile reinforced soils is very much dependent on the properties of the geomaterials and the interface frictional behavior between the geotextile and these materials. Most of these models developed to describe the behavior of these materials are based upon classical theory of elastic-plastic solids. This theory, originally developed for metals to model their behavior, was subsequently modified by adding the effect of pressure dependent yielding and the possibility of plastic volume changes to describe the properties of soils (Collins 2005).

Juran et al. (1988) developed a load transfer model assuming an elasto-plastic strain hardening behavior for the soil and an elastic-perfectly plastic behavior for the reinforcement. Their model can be used for analysis and design response of reinforcement soil material under triaxial compression loading. The model also allows an evaluation of the effect of various parameters such as dilatancy properties of the soil, extensibility of the reinforcements, mechanical characteristics and their inclination with respect to the failure surface. From their

results it was found that the equivalent friction angle of the reinforced sand is significantly smaller than that of the unreinforced sand. In addition, the reinforcing effect decreases as the applied confining pressure increases. It was concluded that the global shear resistance of the soil material depends upon: a) the limit tension or compression forces in the inclusions, and b) the shearing resistance of the soil mobilized at failure of the inclusion.

Juran et al. (1988) presented the application of their model to the numerical analysis of the direct shear test on sand samples reinforced with different types of tension resisting reinforcements. The effect of the mechanical characteristics and dilatancy properties of the soil, extensibility "elastic modulus" of the reinforcements and their inclination with respect to the failure surface on the response of the reinforced soil material to the direct shear were evaluated in their study. Different types of inclusions, such as steel grids and fibers were used, and they concluded that the dilatancy has a significant effect on the shear strength and on the resistance of low shear displacements of the reinforced sand material. Based on the ratio of $\lambda/\emptyset$ and dilatancy rate $v_{s,}$ the effect of reinforcement can be either positive or negative.

This study focuses on investigation of the effect of the interface friction between geosynthetics and soils on the performance of reinforced pavements. The study also analyzes the influence of pavement layer quality on the performance of reinforced pavements.

1.2 Objectives

The specific objectives of the study are to:

1- Simulate the pavement structure performance under static loadings by using finite element analysis,
2- Study the influence of base layer and subgrade quality on the performance of reinforced pavements, and
3- Investigate the influence of the interface friction on the performance of reinforced pavements.

The finite element program ADINA is used in the analyses.

1.3 Organization of Thesis

This thesis organized into six chapters. Chapter 2 provides a literature review of the models that have been developed to describe the behavior of geosynthetics when used as a reinforcement material in the pavement structure under various types of loads. Chapter 3 provides a description of the finite element model that was developed to simulate the reinforced pavement structure. This chapter also provides a parametric study of different parameters that influence pavement performance. Results and discussions are provided in Chapter 4. The fifth and final chapter presents the summary of the major conclusions and recommendations for further research in this area.

CHAPTER TWO

REINFORCED SOIL IN PAVEMENTS: MECHANISMS AND NUMERICAL MODELS

Flexible pavement systems consist of surface course, base course, and sub-base course layers as shown in Fig. 2.1. The surface course usually is of asphalt, whereas the base course consists of gravels and the sub-base course consists of sands and clays. Numerous studies have been done by researchers to investigate the influence of geosynthetics when used as reinforcement materials in the base course layer of flexible pavements (Hass et al. 1988, Penner. 1985, Davies and Bridle. 1990). These studies have concluded that the performance of flexible pavement improved when geogrid was used as a reinforcement material. This improvement was found to be dependent on many factors such as geosynthetic type, manufacturing process, mechanical properties, placement location, and layering; base course thickness and quality, asphalt concrete (AC) thickness: subgrade type, strength, and stiffness characteristics: and load magnitude and frequency of application (Perkins and Ismeik 1997).

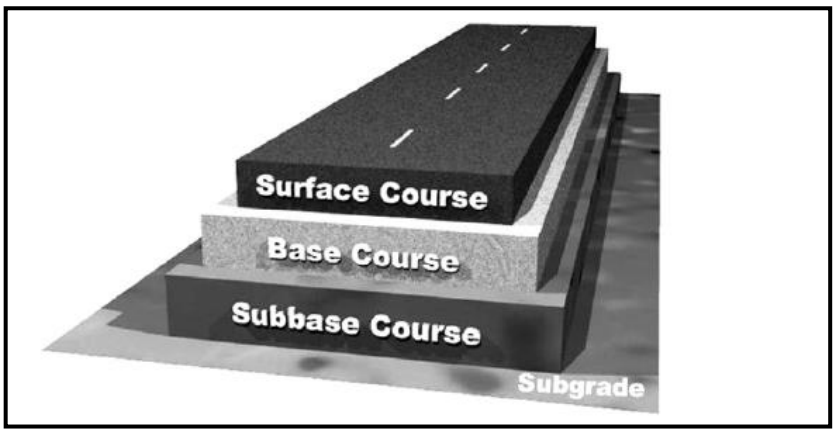

Fig. 2.1: Cross-section of flexible pavement system (Zornberg 2012)

2.1 Mechanisms of Reinforcement in Pavements

Features that improved when geosynthetics were used as a reinforcement material included an increase in pavement service life and a reduction in base course thickness (Perkins and Ismeik 1997). For properly designed sections, the rut depth was reduced by 20 to 58% as well as a reduction in fatigue strain and reflective cracking potential (Brown et al. 1985).

The use of geosynthetics reduced the amount of stresses that are transferred to the subgrade from traffic loads when compared with unreinforced flexible pavement, as shown in Fig. 2.2. Additionally, the geosynthetic reinforcement improved the performance of the pavement through three mechanisms: i) lateral restraint, ii) increased bearing capacity, and iii) tensioned membrane support. These three mechanisms are shown in Fig. 2.3 (Zornberg 2011).

The first mechanism is lateral restraint, shown in Fig. 2.3a. The aggregates in the aggregate layer tend to move horizontally under traffic loads. This phenomenon is restrained by subgrade or geosynthetic reinforcement. The shear stresses due to traffic loads and the aggregate movement result in the development of tensile stresses along the base course. The presence of geosynthetics allows such tensile stresses to be carried by them. Therefore, the interaction between the base aggregate and geosynthetic must be suitable to facilitate such transfer of stresses. The characteristics of the interface between the soil and geosynthetic, including friction and interlocking, will have a dominant effect in contributing to this mechanism (Zornberg 2011).

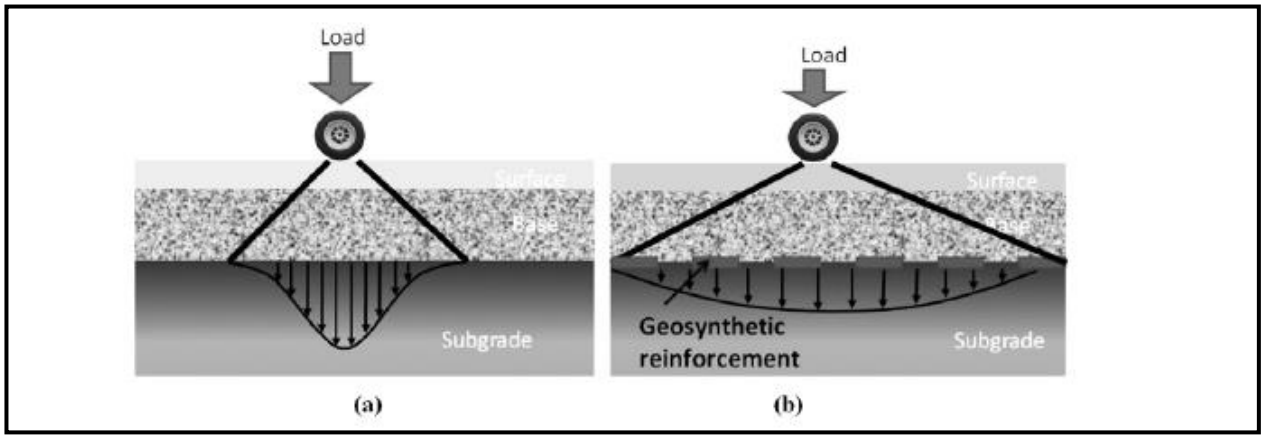

Fig. 2.2: Relative load magnitudes at subgrade layer level for (a) unreinforced flexible pavement and (b) geosynthetic-reinforced flexible pavement (Zornberg 2011).

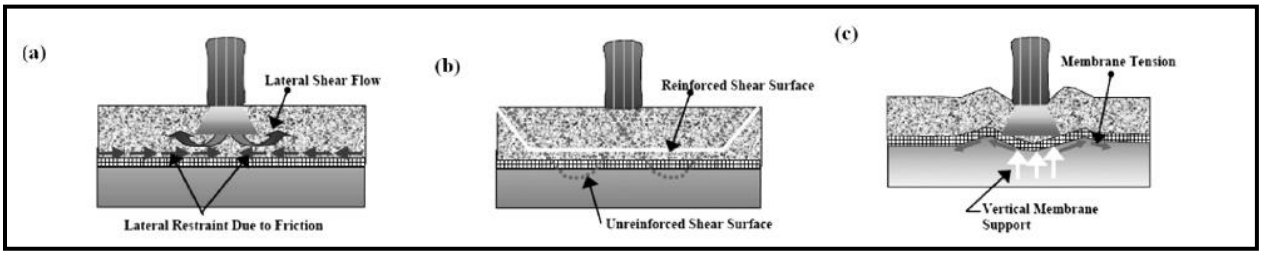

Fig. 2.3: Reinforcement mechanisms induced by geosynthetics (Holtz et al. 1998): (a) Lateral restraint; (b) Increased bearing capacity; and (c) Membrane support (Zornberg 2011).

The second mechanism that is increased is bearing capacity, shown in Fig. 2.3b. The bearing capacity of soil increases when reinforced by geosynthetics because the shearing stresses induced from traffic loads are transferred to geosynthetics. As a result, the subgrade is subjected only to normal stresses. The third mechanism results from tensioned membrane effects, shown in Fig. 2.3c. This phenomenon happens when the aggregate layer deforms under heavy or repeated loading. This deformation will force the geosynthetics layer to deform as shown in Fig. 2.3c. However, the normal stresses in the soil acting on each side of the reinforcement will not be equal if the tensile forces are coincident with an appreciable curvature of the reinforcement. Therefore, the normal stresses that transfer to the subgrade underneath the load will be reduced, which increases the capacity of the road (Brocklehurst 1993).

2.2 Numerical Analyses of Reinforced Pavements

While the above mechanisms are useful to get an understanding of the effects of geosynthetics on pavement layers, numerical analyses are useful to get quantified information on the performance of pavements. The finite element method has been used for pavement analysis for nearly four decades.

Ling and Liu (2003) developed a two dimensional plane strain finite element model using PLAXIS for analysis of the behavior of reinforced asphalt pavement subjected to monotonic loading. They used the program to investigate the effect of using associated and non-associated flow rules for the soil and asphalt materials. The design parameters such as the stiffness of geosynthetic, thickness of asphalt layer, and strength of subgrade foundation on the behavior of a geogrid-reinforced pavement system under monotonic loading were investigated. 6-node elements were used for the sand and asphalt layers. A simple elastic-plastic model employing the Mohr-Coulomb criteria was used to model the soil, while three-node non compression bar elements having linear elastic properties were used to simulate the geosynthetic.

Ling and Liu conducted three types of analysis to simulate loading effects: (i) on sand subgrade foundation alone, (ii) pavement over sand foundation or “unreinforced pavement”, and (iii) geosynthetic- reinforced pavement. In all analyses, the associated and non-associated flow rules were applied for the subgrade foundation. The boundary conditions applied on the model were; the bottom of the mesh was fixed to prevent horizontal and vertical movement, while, the two sides of the mesh were fixed horizontally to allow only vertical movement. The asphalt layer was not fixed.

The difference in results between using associated and non-associated flow rules was found to be small for the pavement system. In addition, the failure load that was obtained from use of an associated flow rule was higher than that used for a non-associated flow rule. In addition, the non-associated flow rule results were more appropriate for simple elastic-plastic analysis of asphalt pavement than for reinforced pavement. Ling and Liu concluded that the load-settlement relationship was improved by increasing the stiffness of geogrid, but there is an upper limit for increasing the stiffness to lead to this improvement. The influence of geosynthetic reinforcement was more significant for weaker subgrades than stiffer subgrades.

Nazzal et al. (2006) developed a two dimensional axisymmetric finite element model to investigate the benefits of reinforcing the base course layer in a flexible pavement structure with geogrid, and to evaluate the effects of different variables, such as the thickness of the base course layer, strength of subgrade soil, and the stiffness of the reinforcement layer on the performance of flexible pavements. Five different reinforced base course thicknesses and three different types of subgrades "weak, moderate, and stiff" were used in their study. Four different biaxial geogrid types were used by placing them at the bottom of the base layer. The pavement system was subjected to cyclic loadings. The parameter that was used to quantify the degree of improvement achieved by the geogrid reinforcement was the depth of rut after application of two million load cycles by using regression models.

Eight-node bi-quadratic axisymmetric quadrilateral elements were used for the subgrade, base, and asphalt concrete layer, while, three-node quadratic membrane elements with thickness of 2 mm was used for the geosynthetic reinforcement. Around 360, 1180, and 2480 elements were used for AC, base course, and subgrade layers respectively. Two types of cyclic loadings were applied on the pavement surface. The Drucker-prager elastic-plastic model was used to

model the base course and subgrade. An elastic-perfectly plastic model was used to simulate the AC layer. In addition, the behavior of the geosynthetic material was modeled using a linear elastic model.

Their study concluded that the permanent deformation (rutting) of pavement sections was reduced when geosynthetic was used. The amount of reduction depended on the subgrade stiffness, geogrid stiffness, and thickness of the base layer. In addition, the effect was found to be more profound for a weaker subgrade than for a stiffer one. The effect of geogrid reinforcement was reduced when the thickness of the base layer increased, and improved when the stiffness of subgrade layer increased.

Howard and Warren (2006) developed an axisymmetric finite element model to analyze data obtained from seventeen heavily instrumented test sections. Triangular elements with either 6 or 15 nodes in all layers were used in their model for asphalt, crushed limestone, compacted subgrade, and natural ground. One dimensional tension elements were used to model the geosynthetic. A linear elastic model was used to capture the behavior of asphalt. A hyperbolic model was used to describe the non-linear stress dependent behavior of the granular materials. The same model was also used to model the non-linear properties of compacted subgrade. The perfectly-plastic Mohr-coulomb model was used to model the properties of natural soil.

Wathugala et al. (1996) developed a two-dimensional axisymmetric finite elements model to investigate the effects of geosynthetic stiffness on pavement behavior. The results of six analyses were compared: Case 1, linear elastic models with geosynthetics (Case 1a, E= 1 Gpa: Case 1b, E= 100 Gpa); Case 2, linear elastic models without geosynthetics; Case 3, elastic-plastic models with geosynthetics (Case 3a, E= 1 Gpa: Case 3b, E= 100 Gpa); Case 4, elastic-

plastic models without geosynthetics. The non-linear behavior of the subgrade under cyclic loads was modeled by using the constitutive model that was developed by Desai et al (1986) and Wathugala and Desai (1993). The base course layer was modeled using the same model that was used to model the subgrade layer. The thickness of the geogrid layer was 2.5 mm, and the bonding between soil and geogrid was not assumed to be full. Wathugala et al. concluded that the amount of permanent rut depth was reduced by close to 20 % for a single cycle of load. The flexural rigidity of the geosynthetic was considered to be the main reason for this reduction.

Several other models have also been carried out to study geosynthetics effects in pavements. A summary of such studies is shown in Table (2.1)

2.3 Experimental Studies on Geosynthetic Pavements

Ling and Liu (2001) conducted a series of tests to investigate the behavior of geosynthetic-reinforced asphalt pavements under monotonic, cyclic, and dynamic loading conditions. The geosynthetic was placed between the asphalt and subgrade soil. Two types of geogrid materials were used: Geogrid A was a biaxial polypropylene geogrid, whereas Geogrid B was a uniaxial polyester geogrid. The stress-strain relationship for geogrids under monotonic and cyclic loadings conducted at 20% of ultimate monotonic strength was presented (Fig. 2.4). Ling et al. concluded that the strength of reinforced asphalt pavements and stiffness (slope of load versus settlement relationship) improved under static and dynamic loading tests. In addition, the settlement that occurred after loading was higher in unreinforced pavement than reinforced pavement. Furthermore, the improvements were more significant for dynamic loading than static loading.

	Author						
	Barksdale et al. (1989)	Burd and Houlsby (1986)	Burd and Brocklehurst (1990)	Burd and Brocklehurst (1992)	Dondi (1994)	Miura et al. (1990)	Wathugala et al. (1996)
Analysis type	Axi-symmetric	Plane strain	Plane strain	Plane strain	Three-dimensional	Axi-symmetric	Axi-symmetric
AC constitutive model	Isotropic, nonlinear elastic	None	None	None	Isotropic, linear elastic	Isotropic, linear elastic	Isotropic elastoplastic, Drucker-Prager
AC thickness (mm)	Variable	None	None	None	120	50	89
Base constitutive model	Anisotropic, linear elastic	Isotropic, elastoplastic, Matusoka	Isotropic, elastoplastic, Matusoka	Isotropic, lastoplastic, Matusoka	Isotropic, elastoplastic, Drucker-Prager	Isotropic, linear elastic	Isotropic, elastoplastic, Drucker-Prager
Base thickness (mm)	Variable	75	300	300	300	150	140
Geosynthetic constitutive model	Linear elastic	Isotropic, linear elastic	Isotropic, linear elastic	Isotropic, linear elastic	Isotropic, linear elastic	Isotropic, linear elastic	Isotropic, elastoplastic, von Mises
Geosynthetic element type	Membrane	Membrane	Membrane	Membrane	Membrane	Truss	Solid continuum
Geosynthetic thickness (mm)	None	None	None	None	None	None	2

Table 2.1: Summary of finite element studies. (Perkins and Ismeik 1997)

Interface elements and model	Linear elastic-perfectly plastic	None	None	Elastoplastic, Mohr-Coulomb	Elastoplastic, Mohr-Coulomb	Linear elastic joint element	None
Subbase constitutive model	None	None	None	None	None	Isotropic, linear elastic	Isotropic, elastoplastic, HiSS δ_o
Subbase thickness (mm)	None	None	None	None	None	200	165
Subgrade constitutive model	Isotropic, non-linear elastic	Isotropic, elastoplastic, von Mises	Isotropic, elastoplastic, von Mises	Isotropic, elastoplastic, von Mises	Isotropic, elastoplastic, Cam-Clay	Isotropic, linear elastic	Isotropic, elastoplastic, HiSS δ_o
Load application	Monotonic	Monotonic, footing width = 75 mm	Monotonic, footing width = 500 mm	Monotonic, footing width = 500 mm	Monotonic, two rectangular areas, 240 mm × 180 mm	Monotonic, 200 mm diameter plate	Single cycle, peak pressure = 725 kPa on a 180 mm diameter plate
Remarks on observed improvement	Base layer could be reduced in thickness by 4 - 18%, greater improvement seen for sections with weak subgrade	Improvement seen after penetration of 4 mm, model overpredicted improvement beyond 4 mm displacement	Improvement seen after penetration of 12 mm, improvement increased with increasing geosynthetic stiffness	Improvement seen after penetration of 25 mm	15 - 20% reduction in vertical displacement, fatigue life of section increased by a factor of 2 - 2.5	5% reduction in vertical displacement, improvement level did not match experimental results	20% reduction in permanent displacement

Table 2.1: Continued. (Perkins and Ismeik 1997)

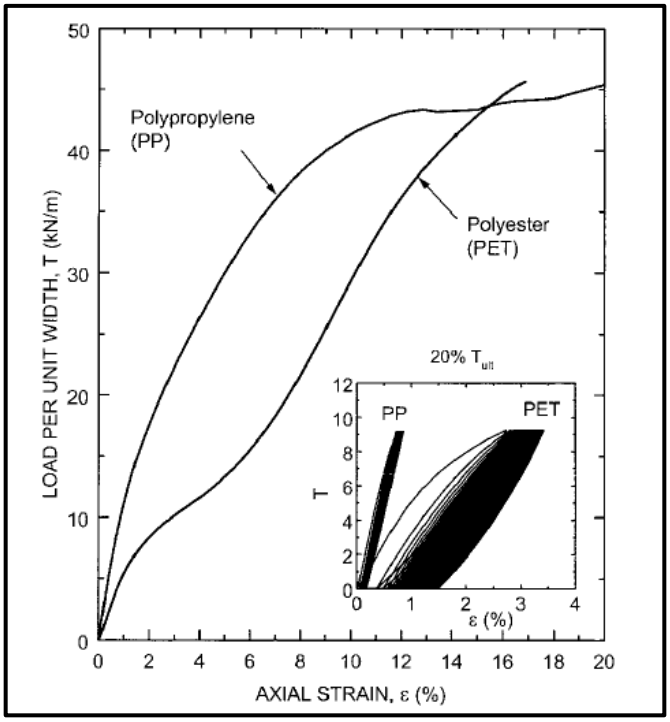

Fig. 2.4: Load-Strain Relationships of Geogrids (Ling et al.1998)

2.4 Interface Frictional Behavior

The interaction coefficients between the reinforcement materials and the fill soil materials around them are critical for design. There are two types of failure: direct sliding failure and pull-out failure associated with reinforced pavements. Therefore design values for these coefficients can be obtained by conducting direct shear and pull-out tests (BOSTD 2007).

From the results of the direct shear test, the direct sliding coefficient, C_{ds}, can be calculated using:

$$C_{ds} = \text{Tan}\,(ø_{ds}) / \text{Tan}\,(ø_{soil}) \qquad (2.1)$$

Where $ø_{ds}$ = the friction angle of soil – geogrid interface; and

$ø_{soil}$ = the friction angle of the soil.

The above formula can be used to calculate the values of C_{ds} for the geogrid reinforced pavement as well as individual granular soil and cohesive soil fill materials. From tests results (BOSTD 2007), the following design values were recommended when geogrids are used as reinforcement materials in the pavement system:

C_{ds} = 0.82 for Granular, Frictional Fills; and

C_{ds} = 0.64 for Cohesive Clay Fills.

Koerner (1994) determined the efficiency of using geotextiles as reinforcement material by conducting direct shear test on various types of geotextiles and fill materials. The efficiency of such materials was defined by:

$$E = (\tan \delta / \tan ø) \tag{2.2}$$

Where E= the efficiency of friction angle mobilization.

The following design values were recommended when geotextiles are used as reinforcement materials in the pavement system:

E = 0.92 for Granular, Frictional Fills; and

E = 0.96 for Cohesive soil.

Yan et al (2010) investigated the factors that affected the performance of geogrids/soil interface for reinforced pavement. The factors that were investigated in their study included fill compaction, water content, and geogrid bore diameter. The effect of these factors on the geogrid/ soil interface was investigated by conducting several experimental on various types of geogrids

and soils. Yan et al (2010) concluded that, when the degree of compaction increased, the friction angle of the interface increased while, when the water content of fill soil increases, the amount of friction angle of interface decreases. For example, when the fill soil was close to saturation, the internal friction angle of reinforced soil decreased by 18.5%. In addition, Yan et al (2010) found that, when the ratio between the soil grain size d_{50} to geogrid bore diameter become close to 0.05, the maximum friction angle of interface achieved.

2.5 Summary

From the literature, it can be concluded that the performance of the pavement structure improved when geosynthetics was used as a reinforcement material. The influence of the geosynthetics in the pavement structure depends on the stiffness of the subgrade layer, and the interface friction between reinforcements and the soil varies significantly.

CHAPTER THREE

FINITE ELEMENT MODEL

Several finite element codes have been used by investigators to simulate pavement structures and to study their behavior for various material conditions and under various types of traffic loadings. Some of the most widely used are ADINA, ABAQUS, PLAXIS, and ILLI_PAVE. Proper use of the finite element method in the solution of boundary value problem requires sound knowledge relating to element size, aspect ratio, material properties, and the type of formulation: There are three types of finite element formulation that have been used in modeling pavements: plane strain, axi-symmetric, and three dimensional. Each formulation has its advantages and disadvantages when used to model pavement behavior. For example, use of two-dimensional plane strain and axi-symmetric formulations are beneficial in terms of time and memory, whereas a three-dimensional model, while more robust, takes much more computational time and memory (Cho et al. 1996).

One of the disadvantages of using two-dimensional plane strain and axi-symmetric formulations for pavement is on the representation of traffic loadings. Traffic loadings in plane strain model are modeled as line loads as shown in Fig. 3.1. On the other hand, traffic loadings in axi-symmetric models are modeled as circular load (Fig. 3.2). The traffic loadings in three-dimensional formulations can be modeled as two semicircles and a rectangle as shown in Fig. 3.3. This enables a better simulation of the pavement field (Cho et al. 1996).

The axi-symmetric model cannot simulate the shoulder conditions or the discontinuity in the pavement structure. A comparison of these models done by Cho et al. suggests that the

results of the plane strain analyses were poor, but that the results of both 3-D and axi-symmetric analyses were acceptable. This study uses an axis-symmetric formulation.

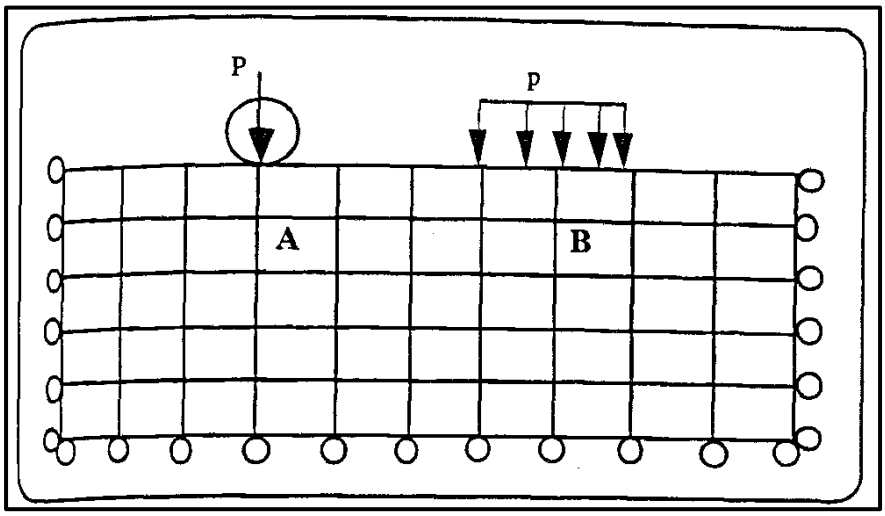

Fig. 3.1: Traffic loading for 2-D plane strain model (Cho et al, 1996).

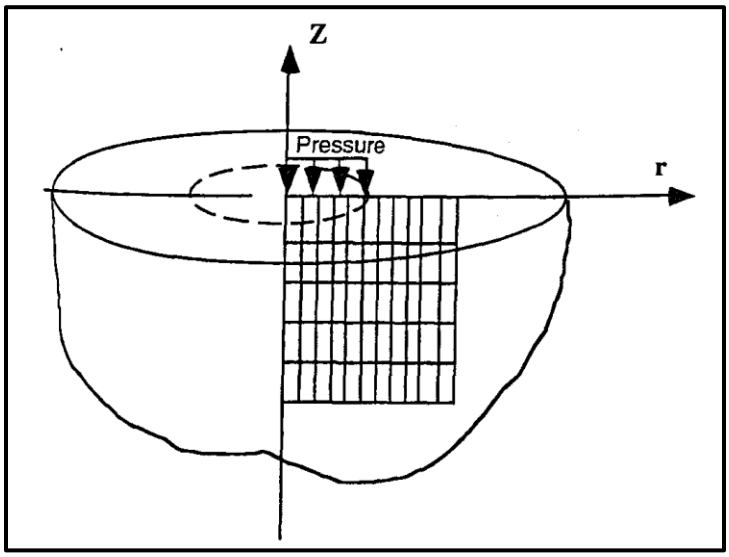

Fig. 3.2: Traffic loading for axisymmetric model (Cho et al, 1996).

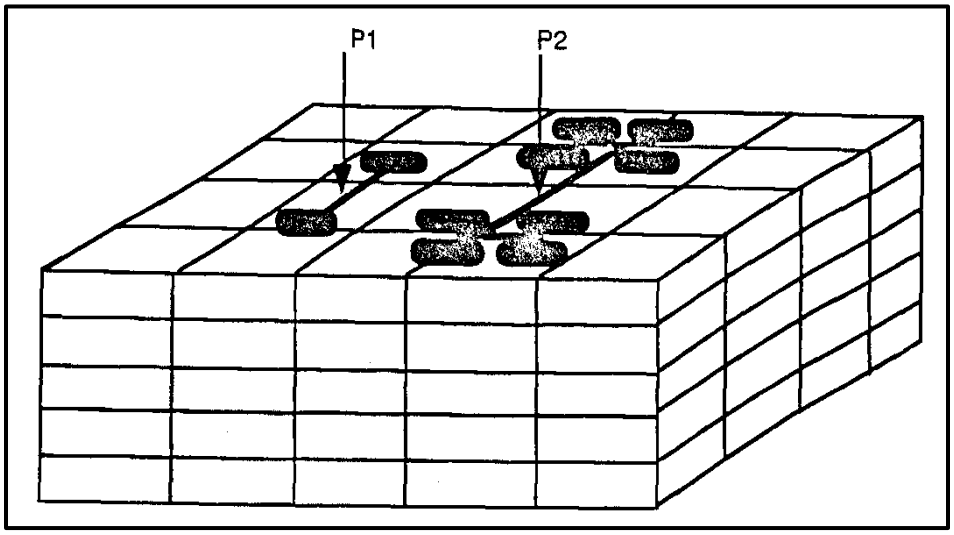

Fig. 3.3: Traffic loading for 3-D model (Cho et al, 1996)

3.1 Finite Element Model

A finite element model was developed using the commercial computer program ADINA to simulate the effects of boundary conditions, layer thickness of pavement on its behavior. Two types of models were created to study the influence of reinforcement on the pavement. The first model is a pavement section without reinforcement and this model is described in section 3.2. The second model is a reinforced pavement section. In this model, the reinforcement material "geosynthetic" was added to the unreinforced model. This model is described in section 3.3.

3.2 Unreinforced FE Model

A two-dimensional axi-symmetric finite element model was developed as shown in Fig. 3.4. A fixed support at the bottom of mesh was used to prevent horizontal and vertical movement. A roller support was used along both sides of the model to prevent the horizontal movement. Three types of layers, AC, Granular base, and Subgrade, were used (Fig. 3.4) to simulate the pavement structure of the road. Elastic material assumptions were used to model the

behavior of AC, Granular base, and Subgrade layer. In addition, eight-node elements were used throughout the mesh. The number of elements that were used for each material were as follows: asphalt concrete (AC), 140; crushed limestone, 404; natural soil, 1512.

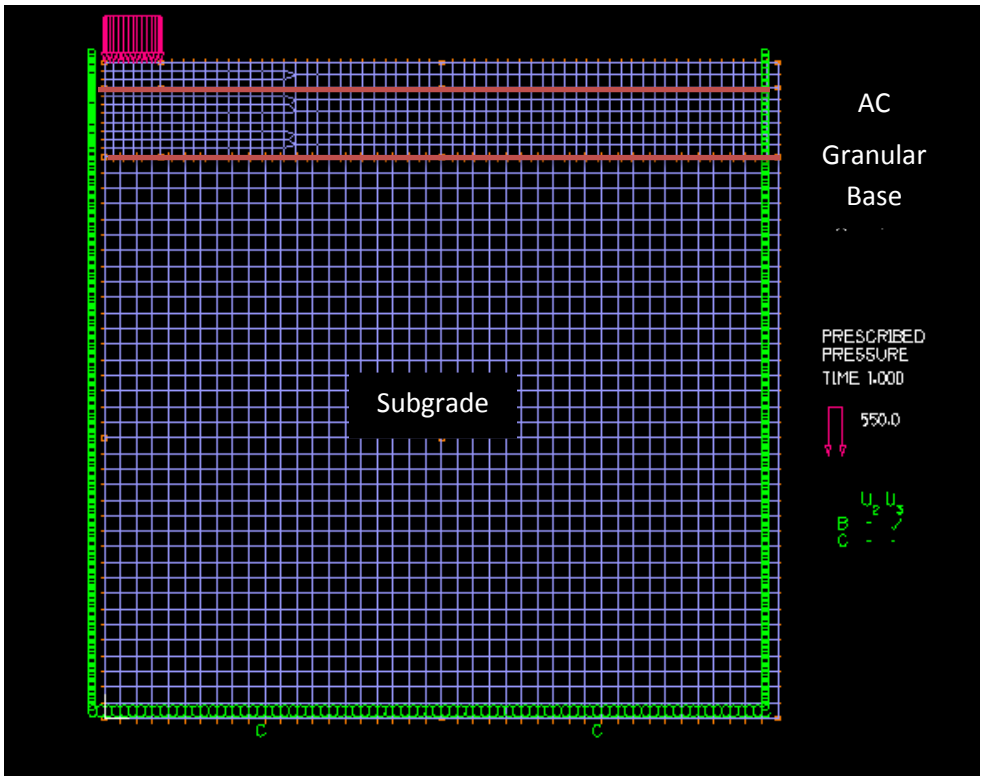

Fig. 3.4: a two-dimensional axisymmetric finite element model

3.3 Geosynthetic Reinforcement FE Model

The second model was developed by adding a layer of geosynthetic reinforcement to the unreinforced model. Eight-node axi-symmetric elements were used to represent the geosynthetic element. The number of elements that were used to model the geosynthetics was 60.

3.4 Loading

A single axial wheel load (40 KN) was applied on the model. This load, however, is assumed to be applied as a static load. It is also assumed that this load is transferred to the pavement surface through the contact pressure of a single tire. Therefore, the amount of pressure that was subjected on the model was taken (550 KPa), which is equal to the amount of tire contact pressure on the road when neglecting the stiffening effect of the tire wall (Saad et al, 2006). The width of the foundation that the wheel pressure was subjected on is 0.25 m. The dimension of the pavement section, layer thicknesses, and the material parameters were taken as those used by Saad et al (2006) in order to be able to compare model results.

3.5 Modeling Interface Friction

One of the key aspects of this study was to investigate the influence of interface friction at the contact surfaces between geosynthetic and pavement layers. This was done by assuming different values of friction coefficients at the contact surfaces between geosynthetic and pavement layers (base and subgrade) as shown in Table (3.1). These values were chosen based on literature review (Eqs 2.1, & 2.2). The first values of friction coefficients, $\mu_1 = 0.362$ and $\mu_2 = 0.294$, are representative of the tangent of the friction angle of the soil-geosynthetic interface. The second values of friction coefficients, $\mu_1 = 0.82$ and $\mu_2 = 0.64$, are representative design values of the friction coefficients between geogrid and granular soil, and between geogrid and cohesive soil, respectively (BOSTD 2007). On the other hand, Koerner (1994) has reported that the appropriate design values for friction coefficients when geotextiles are used as reinforcement material are $\mu_1 = 0.92$ and $\mu_2 = 0.96$.

Geosynthetic Reinforced soil				
Friction Coefficients	μ_1=0; μ_2=0	μ_1=0.392; μ_2=0294	μ_1=0.82; μ_2=0.64	μ_1=0.92; μ_2=0.96

Table (3.1): The geosynthetic friction coefficients

μ_1 is the friction coefficient at the contact surfaces between the geosynthetic and the foundation layer (base); and μ_2 is the friction coefficient at the contact surfaces between the geosynthetic and the subgrade layer.

The influence of these interface friction coefficients was investigated by studying the effect of these parameters on the different types of foundation layers strength, and different types of subgrade layers strength. To achieve the parametric study, the impacts of the geosynthetic reinforcement on four different pavement systems were investigated. The systems analyzed are varying according to the foundation parameters as shown in Table (3.2). Table (3.3) shows the material parameters that were used in this study.

System	Subgrade quality	Base quality
1	Clay	Weak
2	Clay	Strong
3	Silty sand	Weak
4	Silty sand	Strong

Table (3.2): Pavement system analyzed

Layer #	1	2		4	3	
Material	Asphalt-Concrete	Granular Base		Geosynthetics	Subgrade	
		Weak base	Strong base		Silty sand	Clay
Thickness, m	0.1016	0.3048		0.00254	2.5	
Material Model	Linear elastic	Linear elastic		Linear elastic	Linear elastic	
E , KPa	4,134,693	96,793	414,000	4,230,000	50,646	8,280
V	0.3	0.3	0.3	0.35	0.28	0.25

Table (3.3): Material parameters

CHAPTER FOUR

RESULTS AND DISCUSSIONS

4.1 Results and Discussions

The cross-sectional view of the pavement layers and the location of the element for which detailed information is studied are shown in Fig. 4.1. The parameters studied are the vertical surface deflection along the top surface (1-2) and the horizontal displacement along the interface between base and subgrade. The maximum values of vertical surface deflection and horizontal displacement are studied in detail in sections 4.4 and 4.5.The variations of these parameters along surfaces for different reinforced pavement system are shown in Figs. 4.2-4.29.

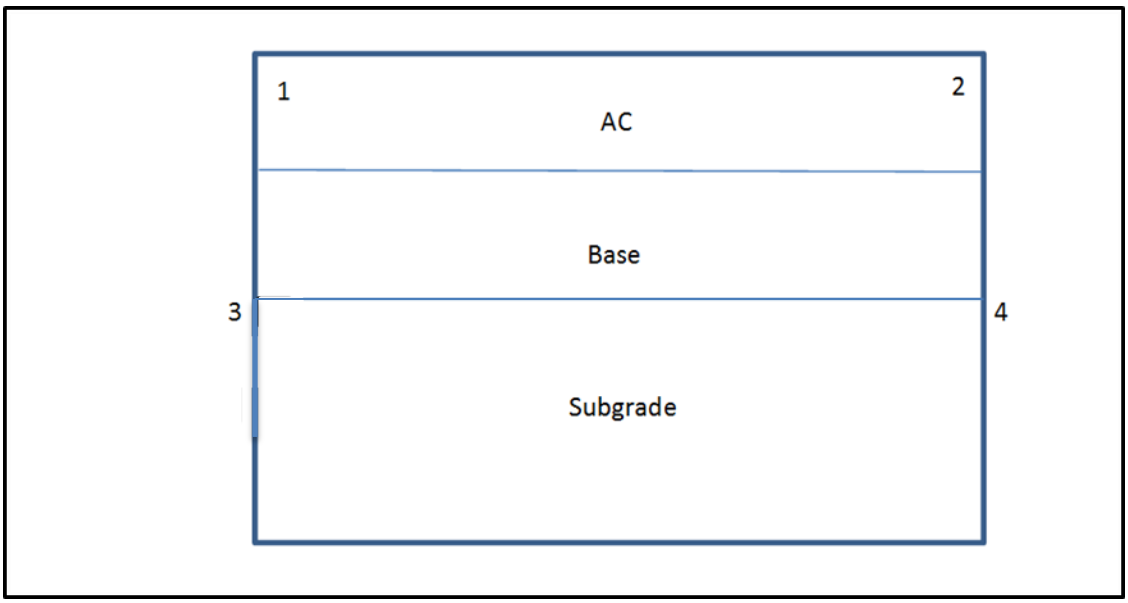

Fig. 4.1: Locations covered in the finite element simulations.

4.2 Distribution of Vertical Deflection

Figs. 4.2 to 4.9 show that the distribution of the vertical surface deflection along the pavement's cross-section for the unreinforced pavement is extended along the asphalt layer, the base layer, and part of subgrade layer. This distribution is changed when the strength of subgrade increases (Figs. 4.10 to 4.15). The amount of maximum vertical deflection decreases when the amount of interface friction coefficients μ increases (Figs. 4.3 to 4.15). The highest reduction occurs when the interface friction coefficients equal μ_1=0.96; and μ_2=0.92 (Figs 4.6, 4.9, 4.12, and 4.15). In the following, the figures are presented first and since the pattern of observation is similar, the discussion of the vertical surface deflection results is presented in section 4.4.

Fig. 4.2 shows the distribution of vertical deflection along the pavement cross-section for the case of an unreinforced pavement system having *weak base layer* and *clayey subgrade layer*.

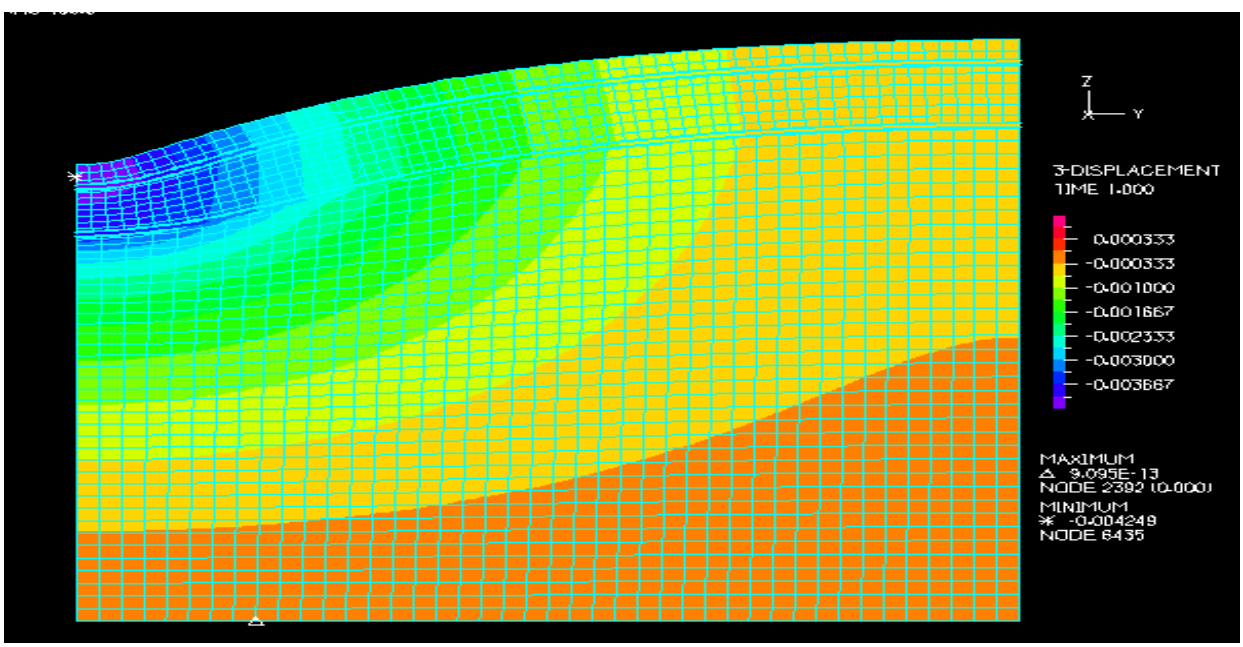

Fig. 4.2: The distribution of vertical deflection along the pavement cross-section for case of an unreinforced pavement.

Figs. 4.3 – 4.6 show the distribution of vertical deflection along the pavement cross-section for the case of a reinforced pavement system for the same *weak base layer and clayey subgrade*, for various values of friction coefficients at the interface between geosynthetic and pavement layers.

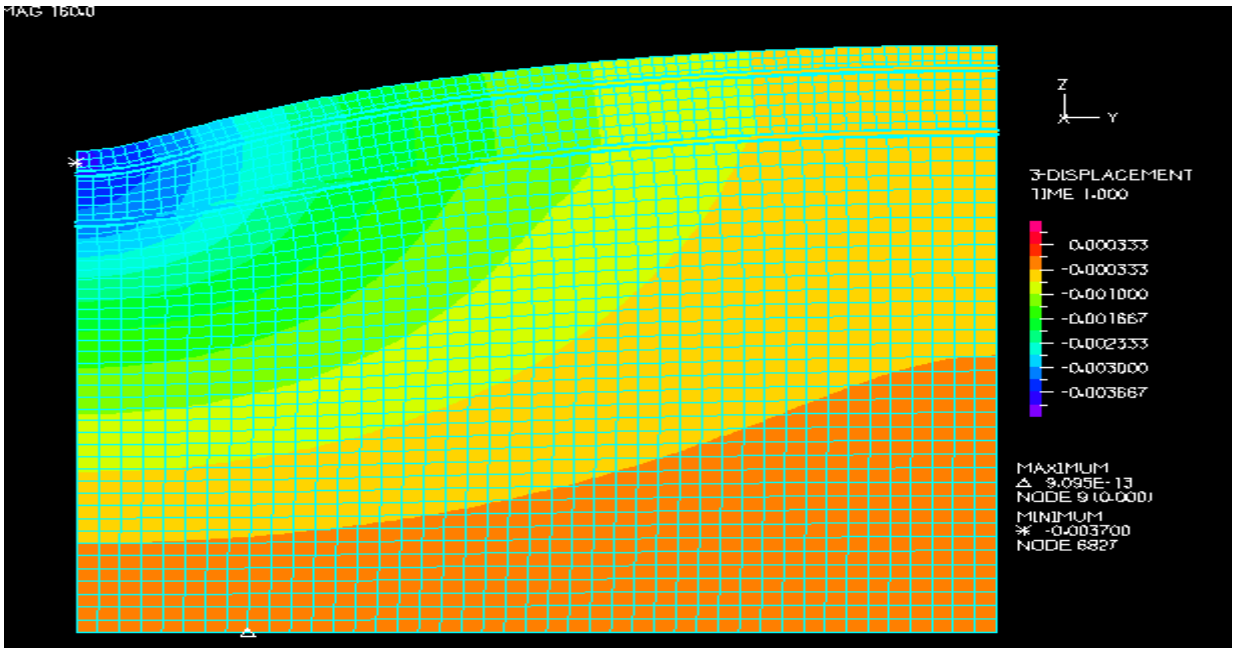

Fig. 4.3: The distribution of vertical deflection along the pavement cross-section for case of a reinforced pavement μ_1=0; and μ_2=0

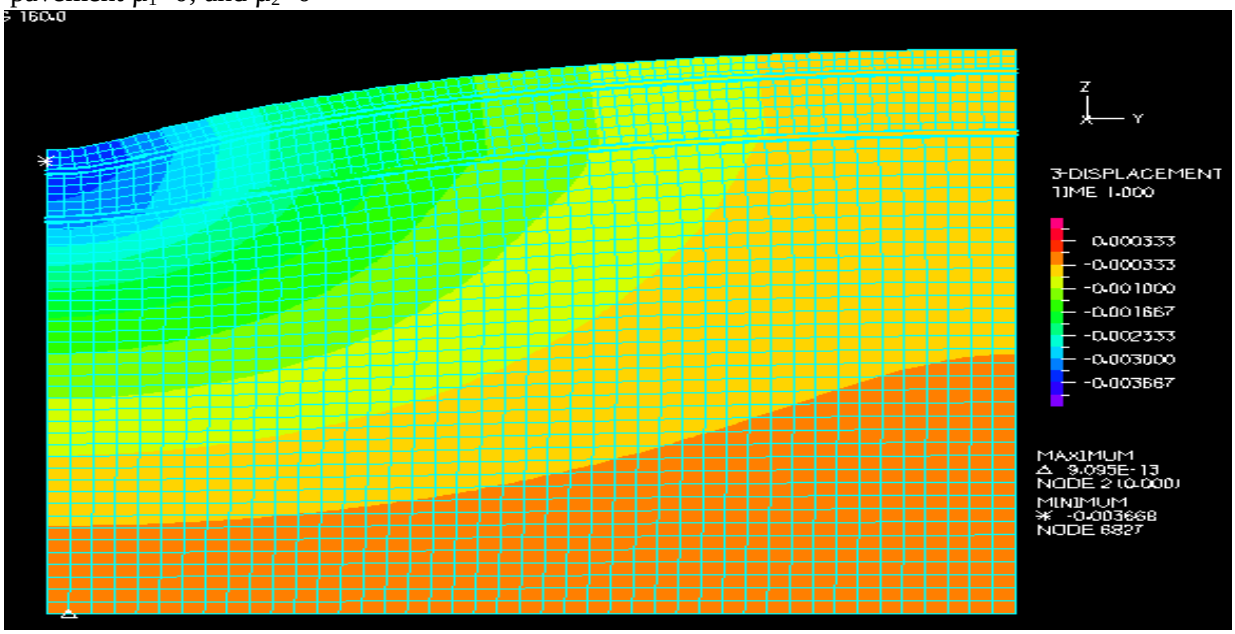

Fig. 4.4: The distribution of vertical deflection along the pavement cross-section for case of a reinforced pavement μ_1=0.392; and μ_2=0.294

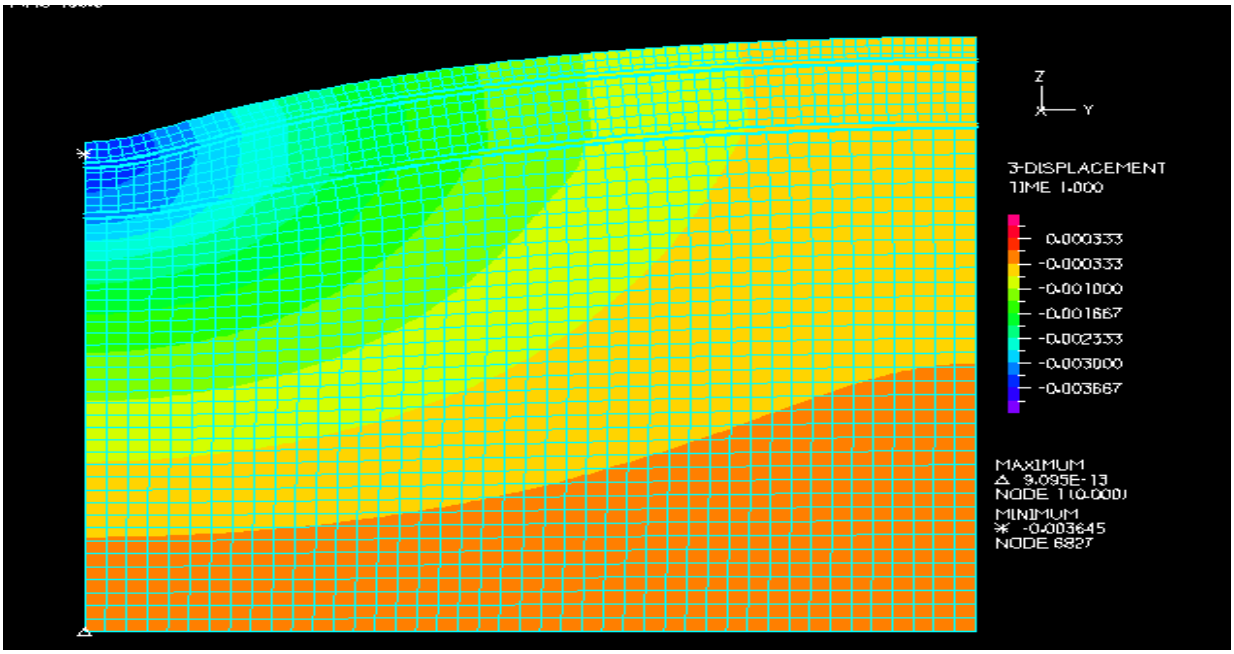

Fig. 4.5: The distribution of vertical deflection along the pavement cross-section for case of a reinforced pavement μ_1=0.82; and μ_2=0.64

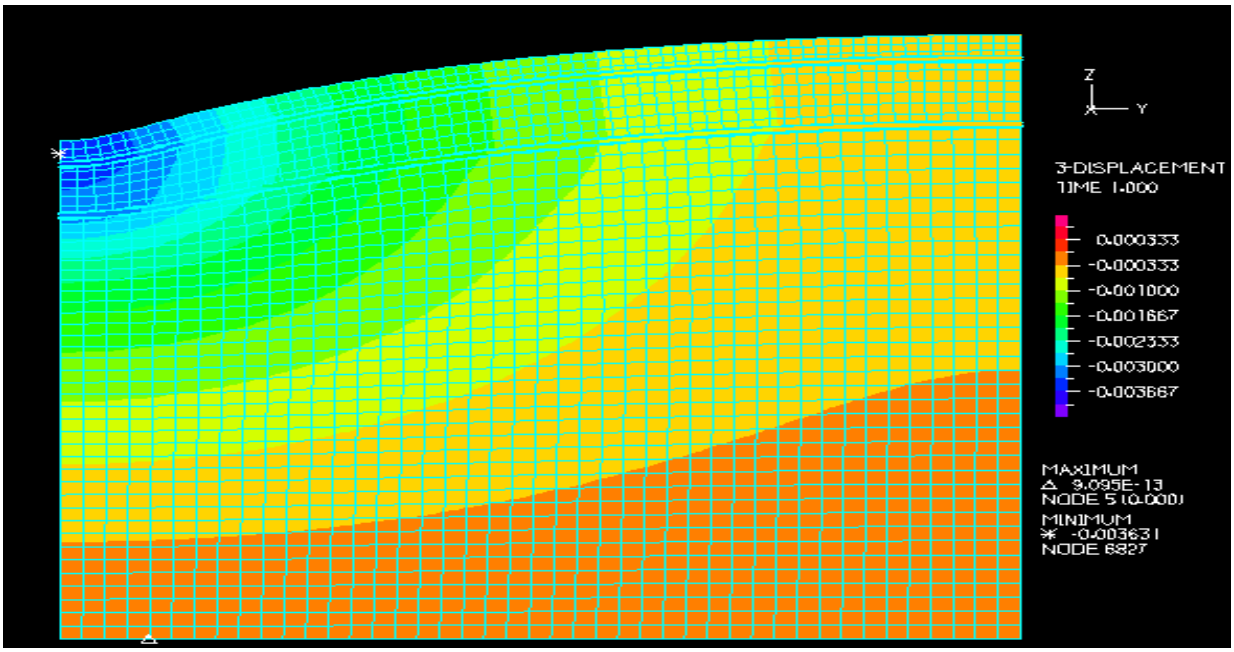

Fig. 4.6: The distribution of vertical deflection along the pavement cross-section for case of a reinforced pavement μ_1=0.96; and μ_2=0.92

Fig. 4.7 shows the distribution of vertical deflection along the pavement cross-section for the case of an unreinforced pavement system having *strong base layer* and *clayey subgrade*.

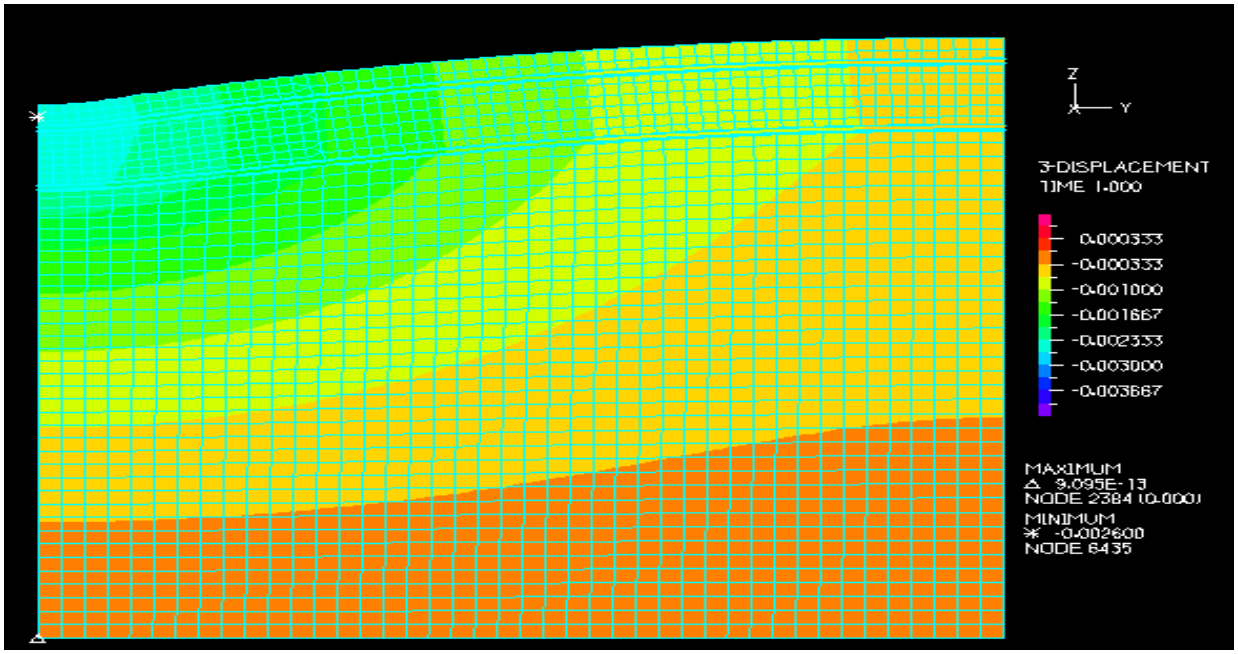

Fig. 4.7: The distribution of vertical deflection along the pavement cross-section for case of an unreinforced pavement having strong base and clayey subgrade layer

Figs. 4.8 and 4.9 show the distribution of vertical surface deflection along the pavement cross-section for the case of a reinforced pavement system having *strong base layer* and *clayey subgrade* layer for various values of interface friction.

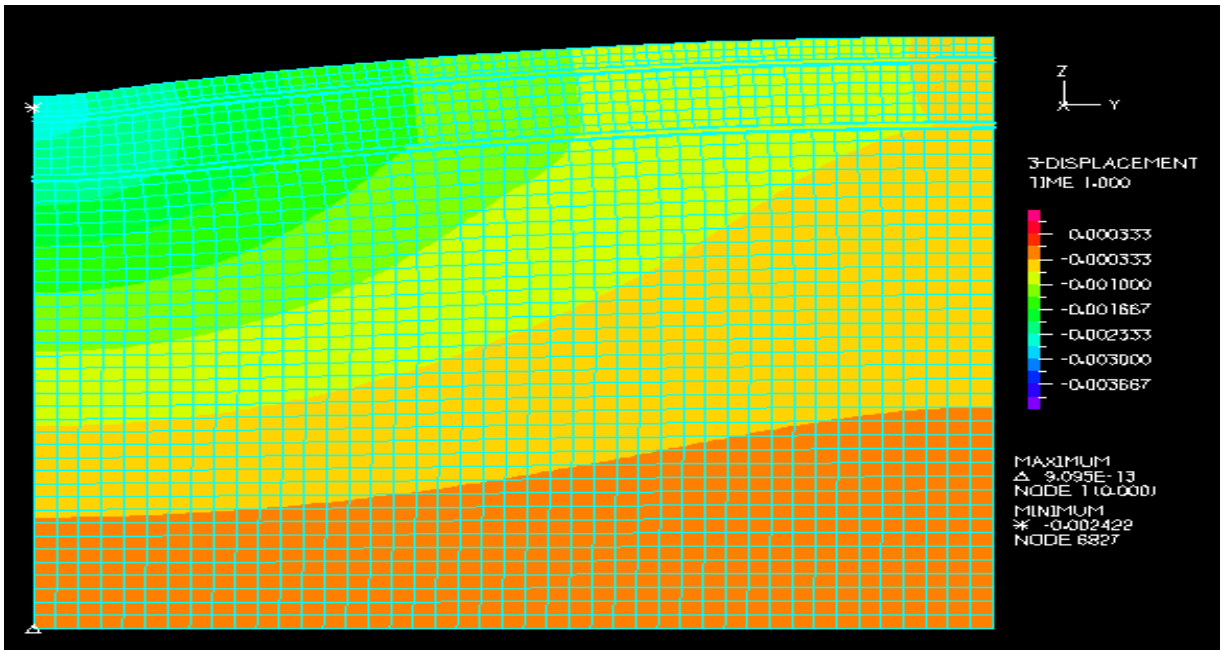

Fig. 4.8: The distribution of vertical deflection along the pavement cross-section for case of a reinforced pavement μ_1=0; and μ_2=0 having strong base and clayey layer

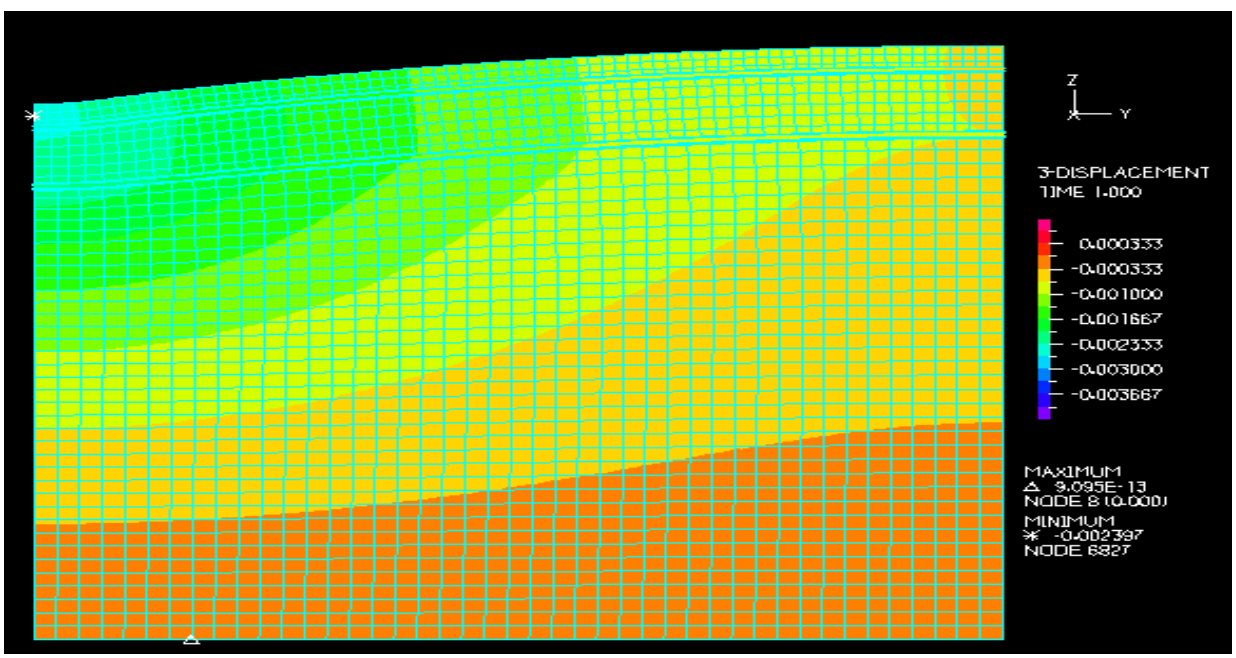

Fig. 4.9: The distribution of vertical deflection along the pavement cross-section for case of a reinforced pavement μ_1=0.92; and μ_2=0.96 having strong base and clayey layer

Fig. 4.10 shows the distribution of vertical deflection along the pavement cross-section for the case of an unreinforced pavement system having *weak base layer* and *silty sand subgrade layer*.

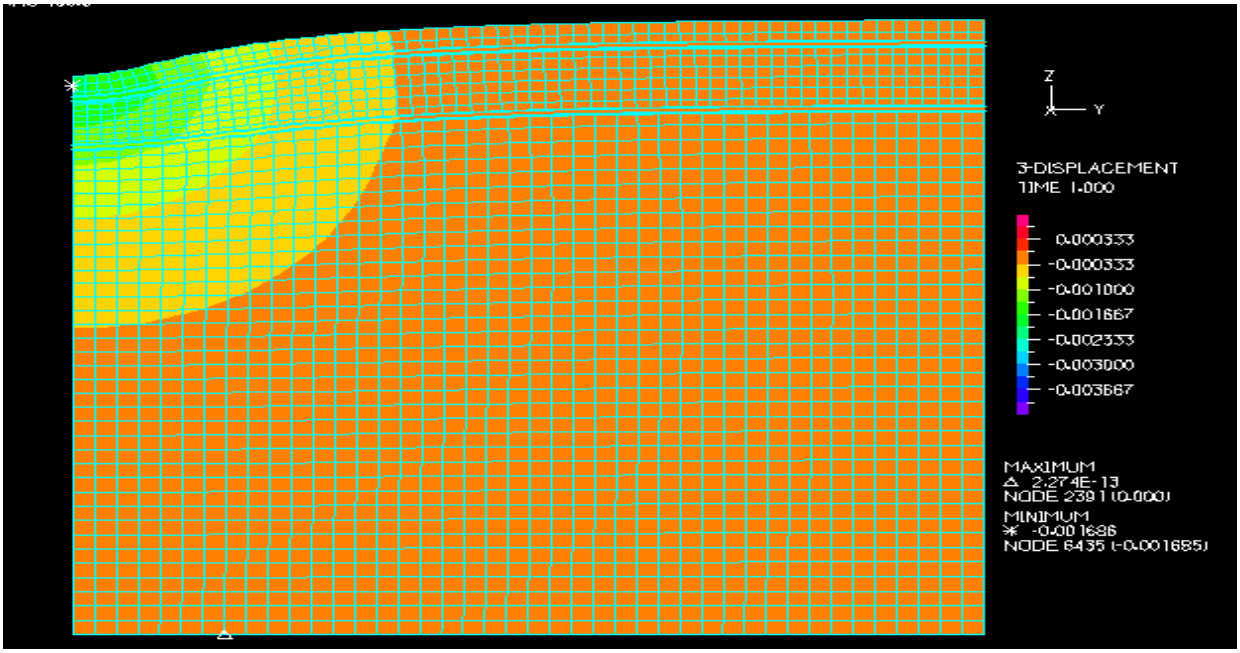

Fig. 4.10: The distribution of vertical deflection along the pavement cross-section for case of an unreinforced pavement having weak base and silty subgrade layer

Figs. 4.11 and 4.12 show the distribution of vertical surface deflection along the pavement cross- section for the case of a reinforced pavement system having *weak base layer* and *silty sand subgrade* layer for various values of interface friction.

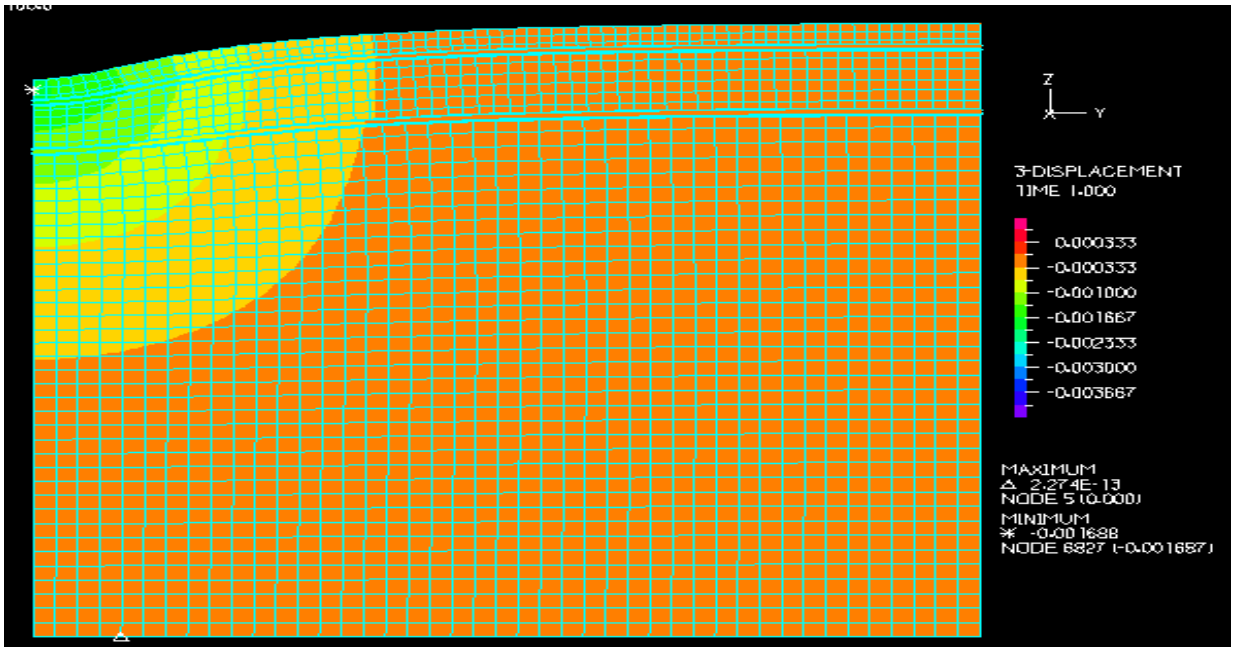

Fig. 4.11: The distribution of vertical deflection along the pavement cross-section for case of a reinforced pavement μ_1=0; and μ_2=0 having weak base and silty sand layer

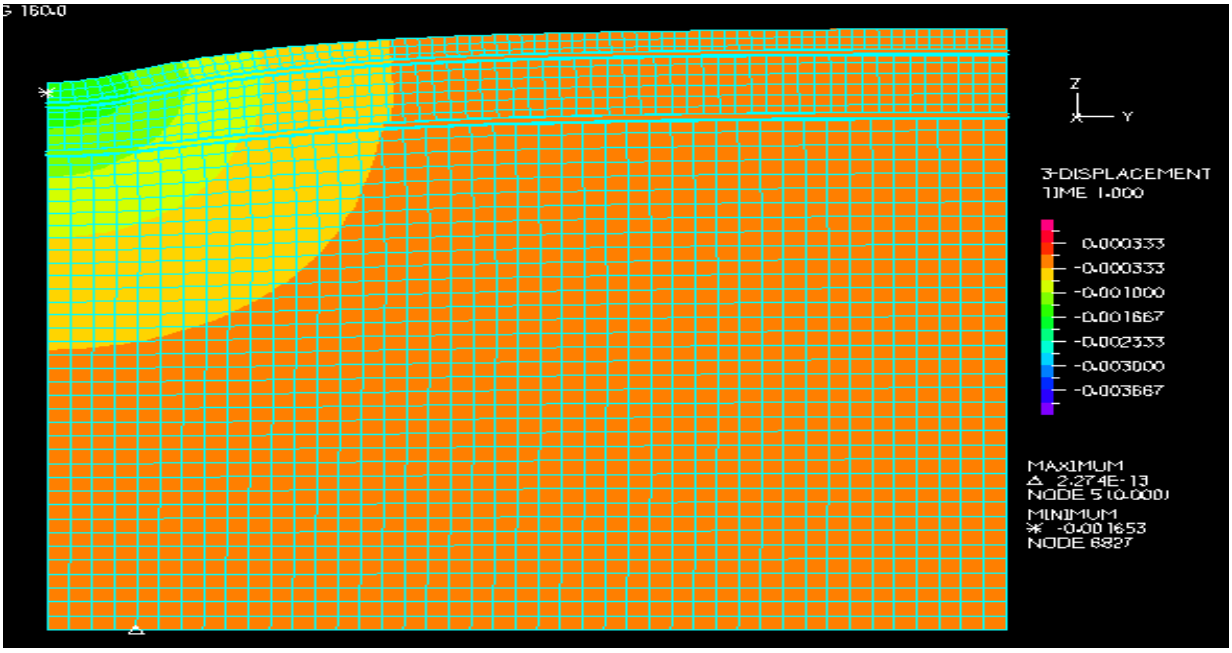

Fig. 4.12: The distribution of vertical deflection along the pavement cross-section for case of a reinforced pavement μ_1=0.92; and μ_2=0.96 having weak base and silty sand layer

Fig. 4.13 shows the distribution of vertical deflection along the pavement cross-section for the case of an unreinforced pavement system having strong base layer and *silty sand subgrade layer*.

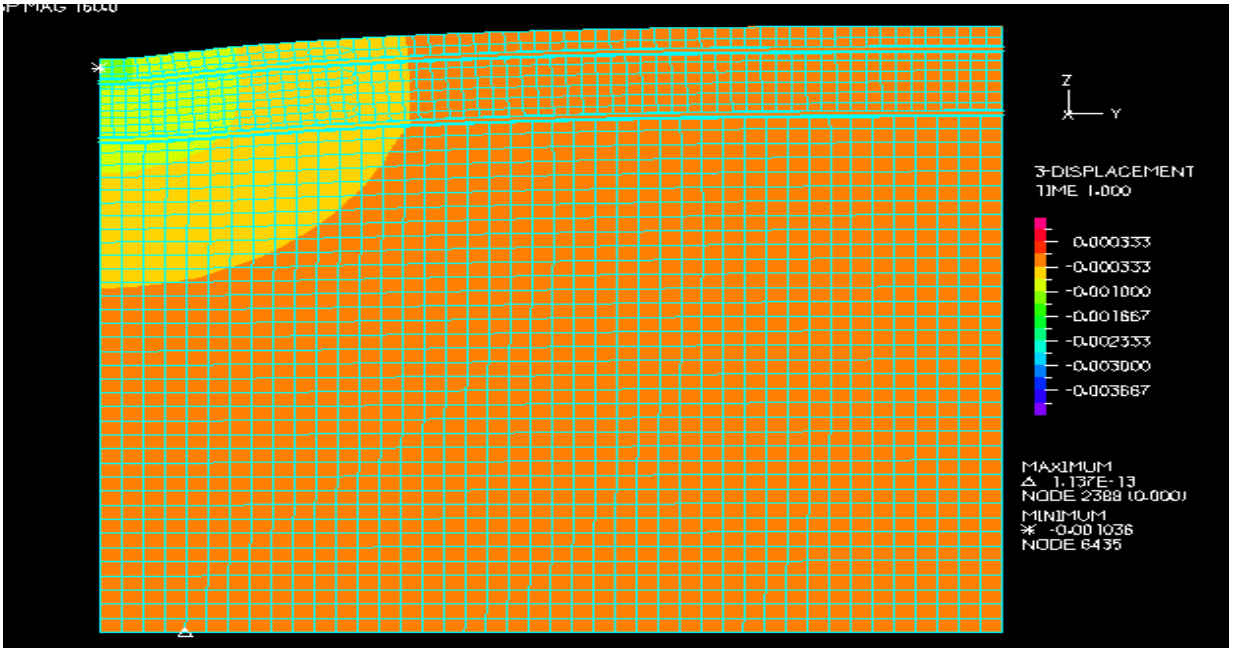

Fig. 4.13: The distribution of vertical deflection along the pavement cross-section for case of an unreinforced pavement having strong base and silty subgrade layer

Figs. 4.13 and 4.14 show the distribution of vertical surface deflection along the pavement section for the case of a reinforced pavement system having *strong base layer* and *silty sand subgrade* layer for various values of interface friction.

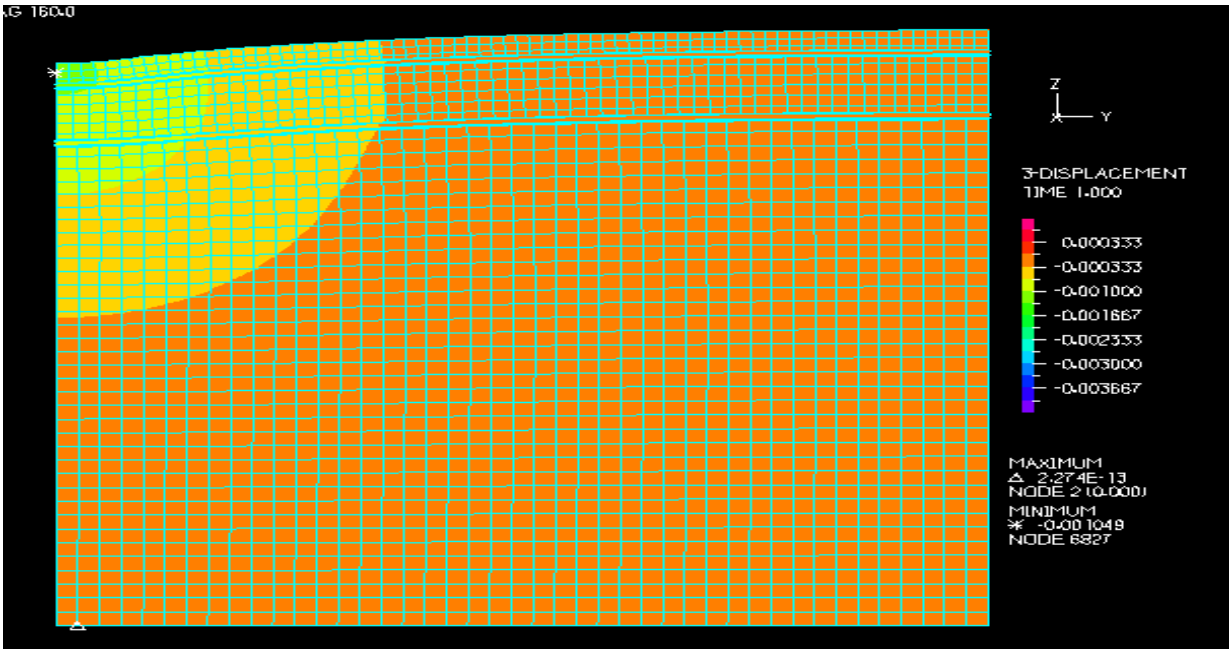

Fig. 4.14: The distribution of vertical deflection along the pavement cross-section for case of a reinforced pavement μ_1=0; and μ_2=0 having strong base and silty sand layer

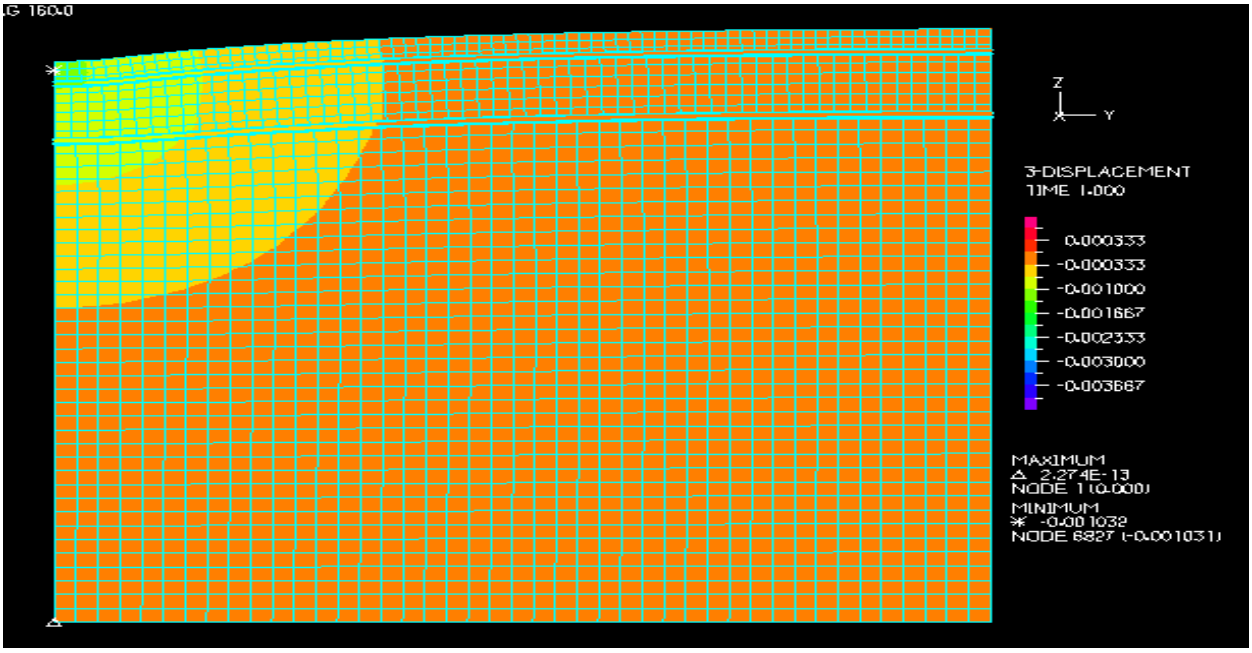

Fig. 4.15: The distribution of vertical deflection along the pavement cross-section for case of a reinforced pavement μ_1=0.92; and μ_2=0.96 having strong base and silty sand layer

It can be concluded from the observations of Figs 5.2-5.15 that the highest reduction of the vertical surface deflection occurs when the friction coefficients equal μ_1= 0.92; μ_2 = 0.96 between the geosynthetic and the foundation layer, and between the geosynthetic and the subgrade respectively. Additionally, the influence of the geosynthetic decreases when the strength of subgrade layer increases.

4.3 Distribution of Horizontal Displacement

Figs 4.16 to 4.29 show that the distribution of the horizontal displacement along the pavement's cross-section occurs as circles for the case of an unreinforced pavement around the interface between the base layer and the subgrade layer. However, when the geosynthetic is placed between the base layer and the subgrade layer the distribution of horizontal displacement changed (Figs. 4.17 to 4.19). The distribution of horizontal displacement further changes when the friction coefficients increase. Figs 4.17, 4.22, 4.25, and 4.28, show that the maximum horizontal displacement occurs at the interface surface between geosynthetic and the base layer. The discussion of the horizontal displacement results is presented in section 4.4.

Fig. 4.16 shows the distribution of horizontal displacement along the pavement cross-section for the case of an unreinforced pavement system having *weak base layer* and *clayey subgrade layer*.

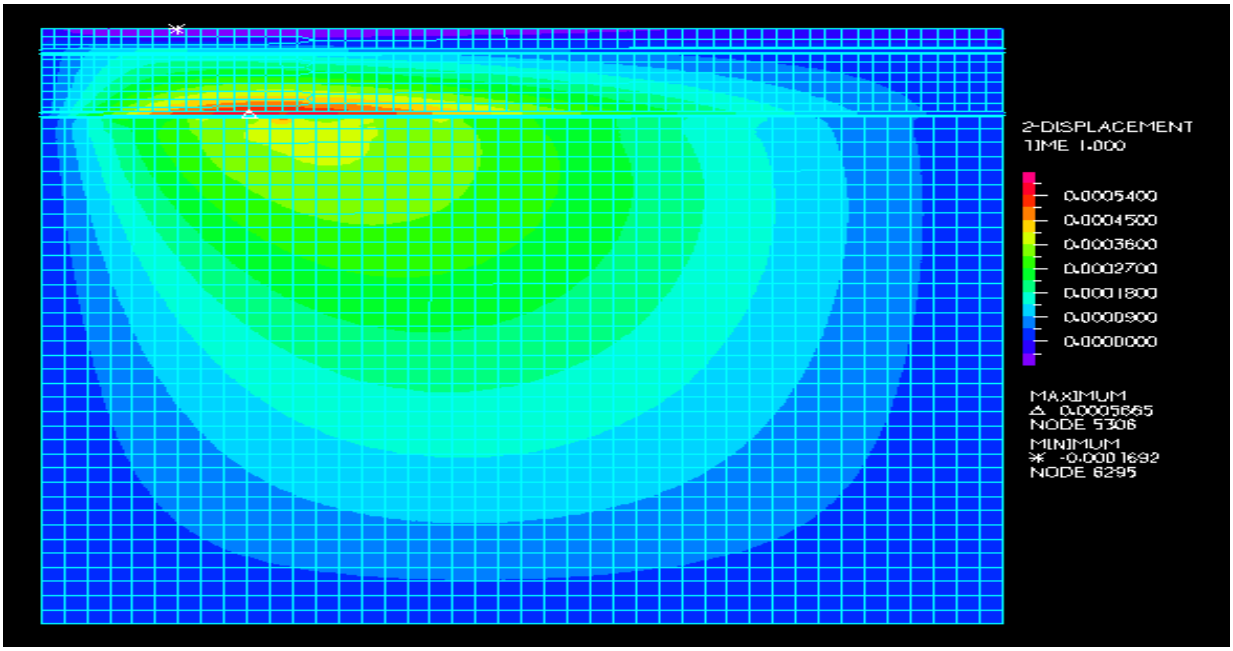

Fig. 4.16: The distribution of horizontal displacement along the pavement cross-section for case of an unreinforced pavement having weak base and clayey subgrade layer

Figs. 4.17 – 4.20 show the distribution of horizontal displacement along the pavement cross-section for the case of a reinforced pavement system having *weak base layer* and *clayey subgrade*, for various values of interface friction at the interface between geosynthetic and pavement layers.

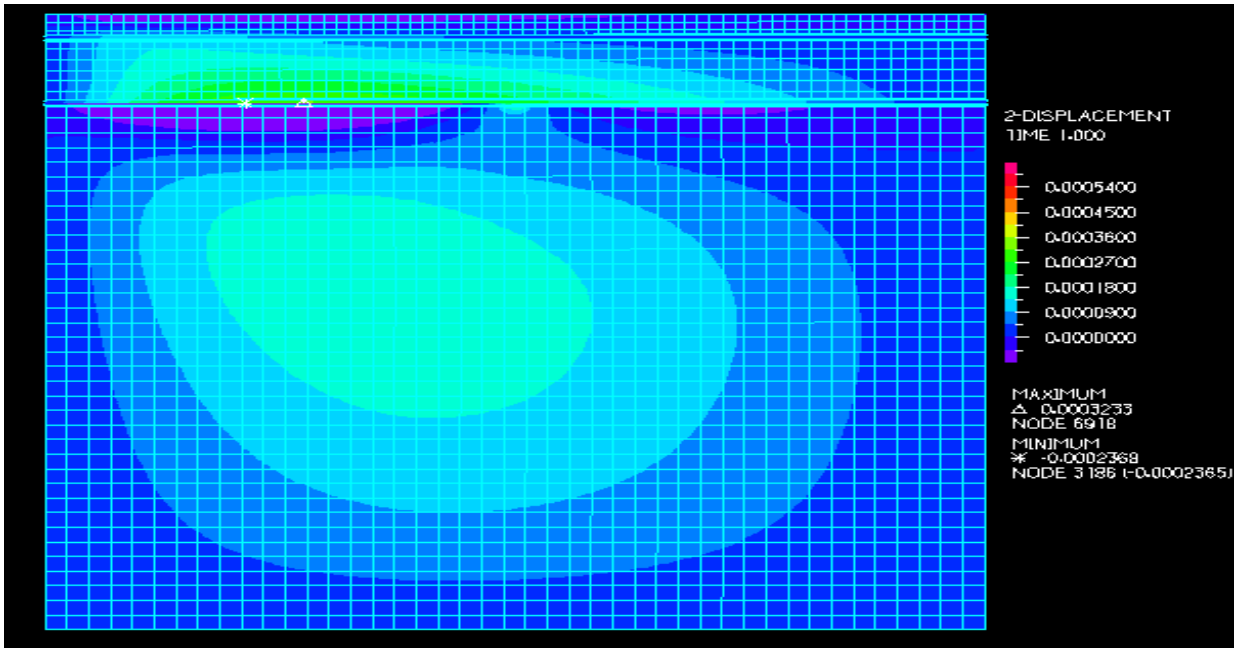

Fig. 4.17: The distribution of horizontal displacement along the pavement cross-section for case of a reinforced pavement μ_1=0; and μ_2=0 having weak base and clayey subgrade layer

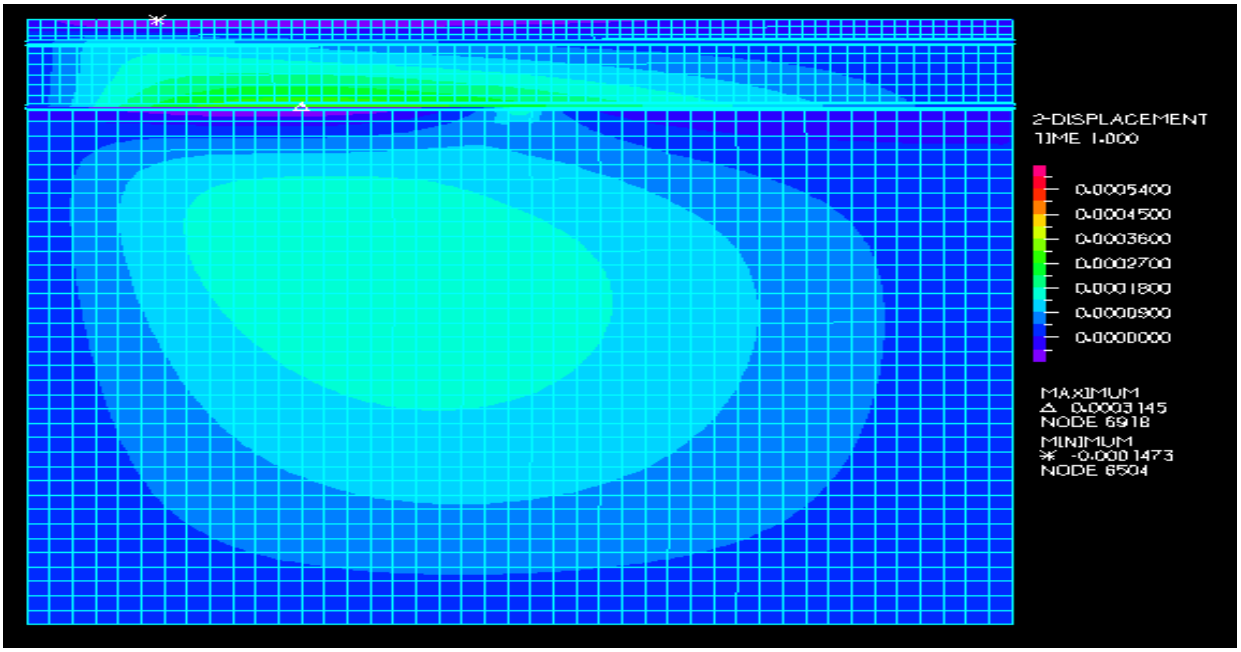

Fig. 4.18: the distribution of horizontal displacement along the pavement cross-section for case of a reinforced pavement μ_1=0.392; and μ_2=0.294 having weak base and clayey subgrade layer

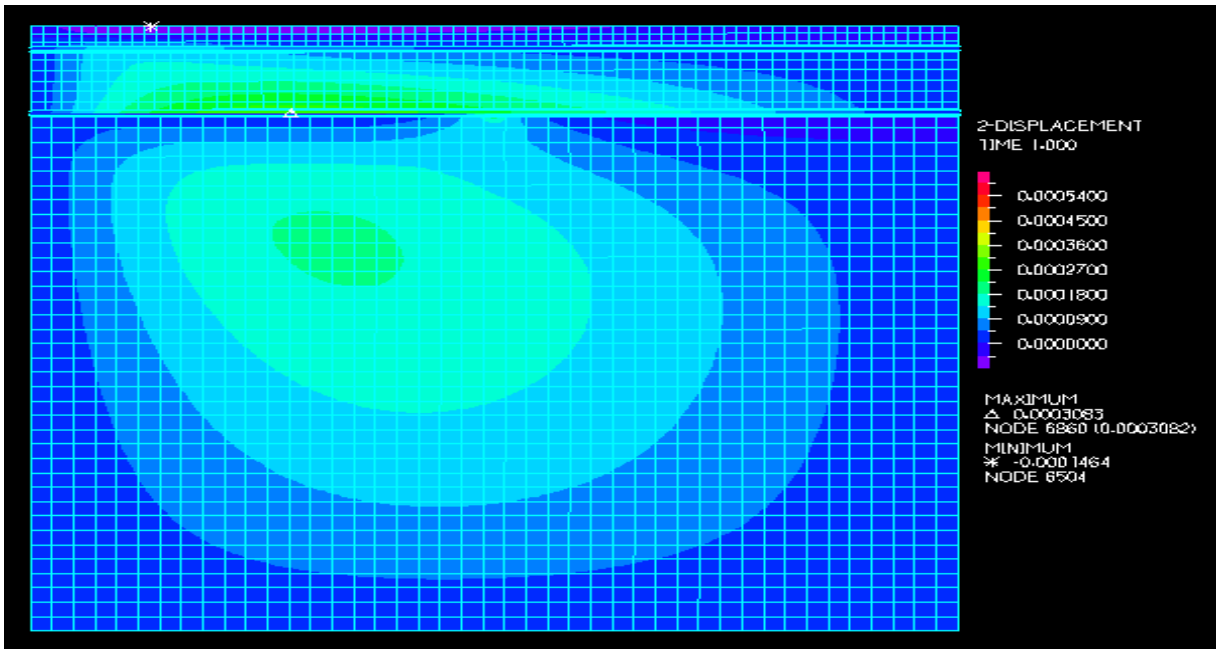

Fig. 4.19: The distribution of horizontal displacement along the pavement cross-section for case of a reinforced pavement μ_1=0.82; and μ_2=0.64 having weak base and clayey subgrade layer

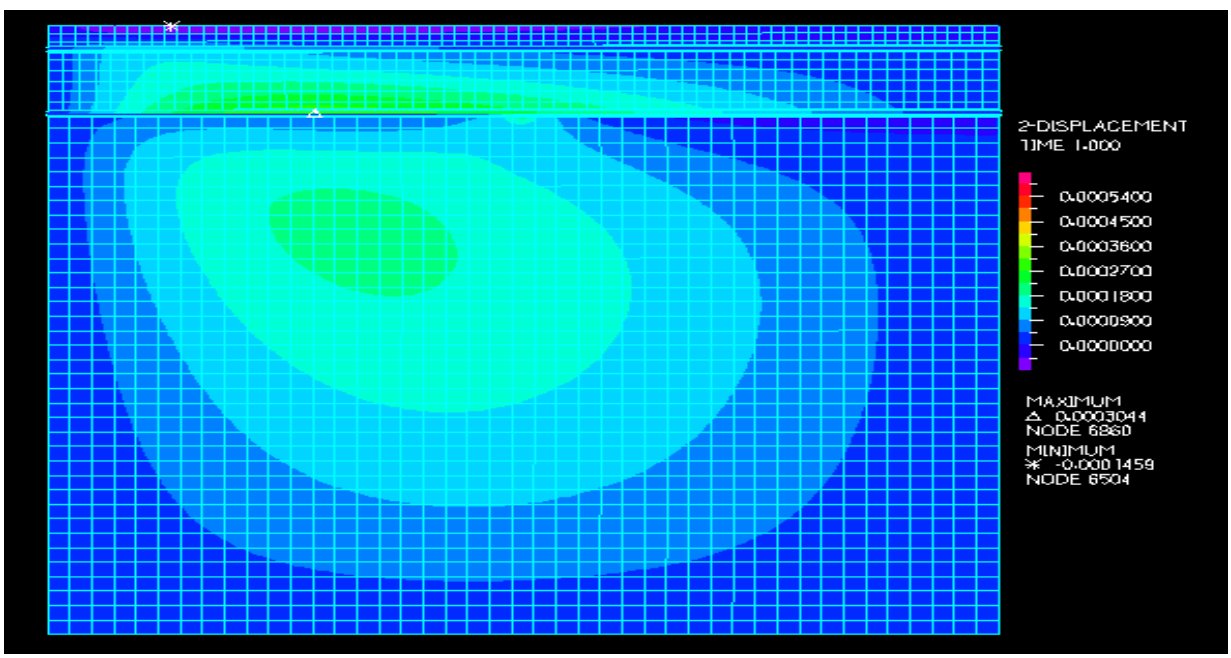

Fig. 4.20: The distribution of horizontal displacement along the pavement cross-section for case of a reinforced pavement μ_1=0.92; and μ_2=0.96 having weak base and clayey subgrade layer

Fig. 4.21 shows the distribution of horizontal displacement along the pavement cross-section for the case of an unreinforced pavement system having *strong base layer* and *clayey subgrade layer*.

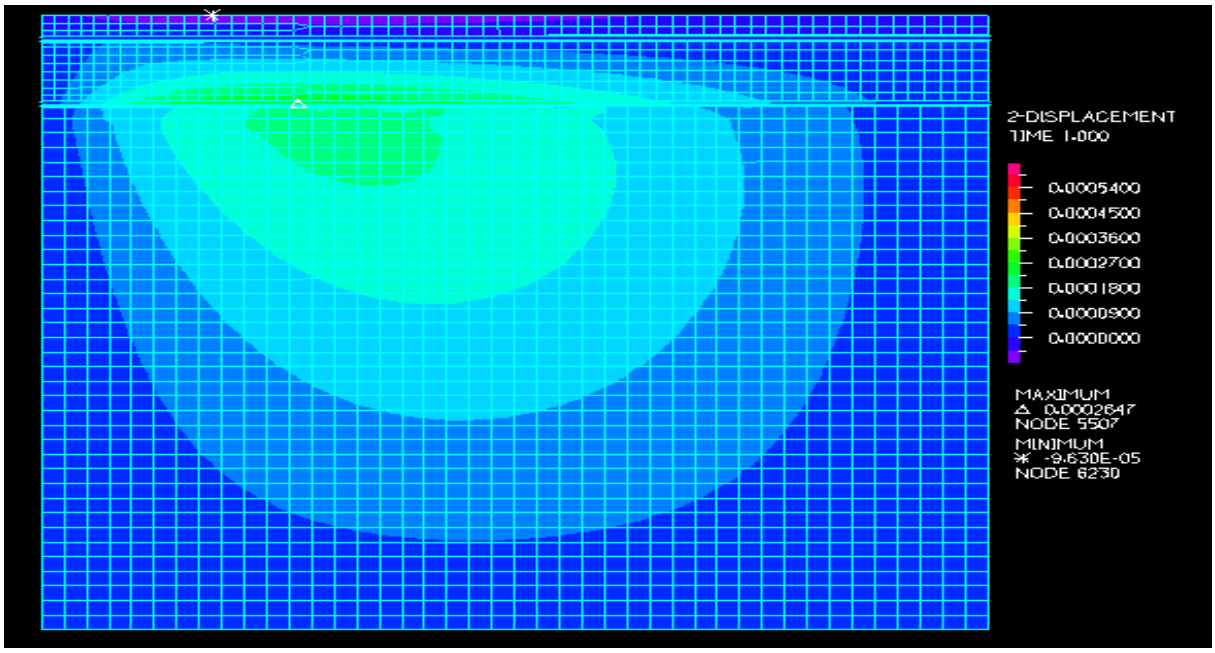

Fig. 4.21: The distribution of horizontal displacement along the pavement cross-section for case of an unreinforced pavement having strong base and clayey subgrade layer

Figs. 4.21 and 4.22 show the distribution of horizontal displacement along the pavement cross-section for the case of a reinforced pavement system having *strong base layer* and *clayey subgrade layer* for various values of interface friction.

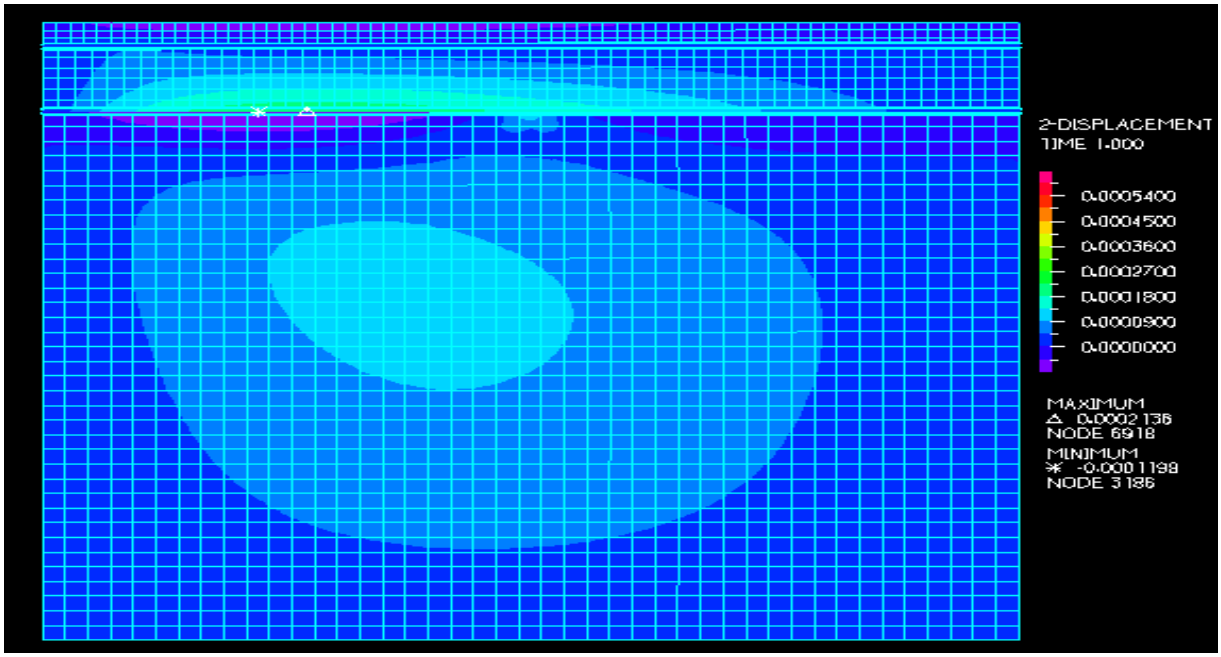

Fig. 4.22: The distribution of horizontal displacement along the pavement cross-section for case of a reinforced pavement μ_1=0; and μ_2=0 having strong base and clayey subgrade layer

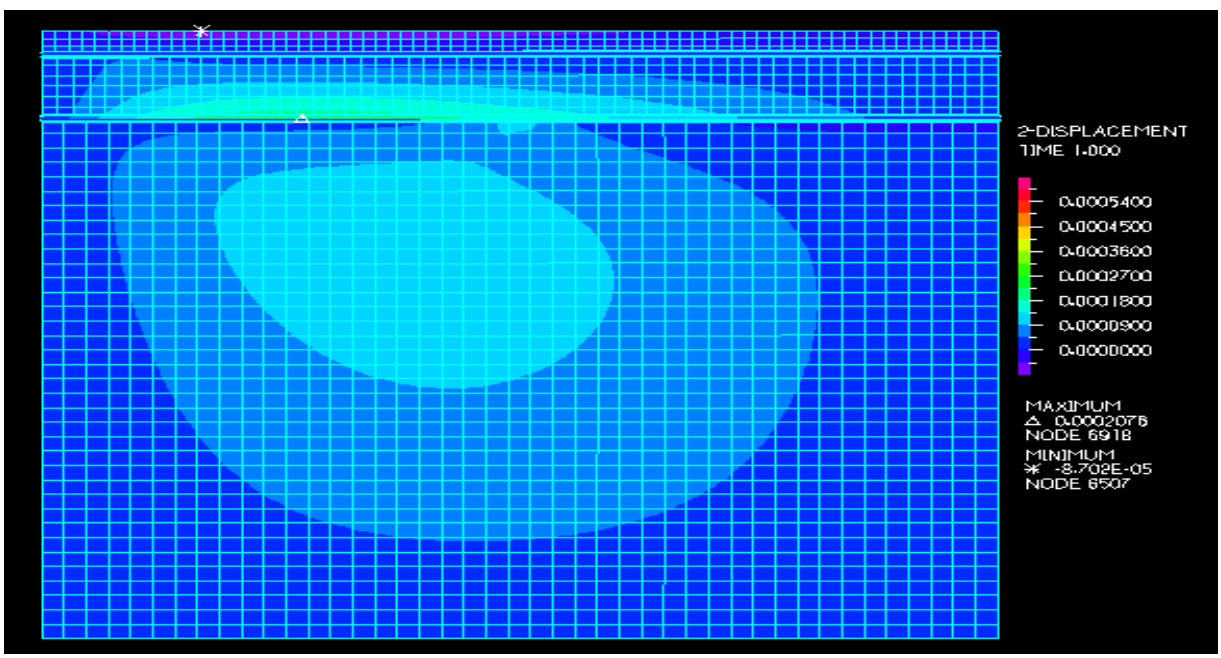

Fig. 4.23: The distribution of horizontal displacement along the pavement cross-section for case of a reinforced pavement μ_1=0.92; and μ_2=0.96 having strong base and clayey subgrade layer

Fig. 4.24 shows the distribution of horizontal displacement along the pavement cross-section for the case of an unreinforced pavement system having *weak base layer and silty subgrade layer*.

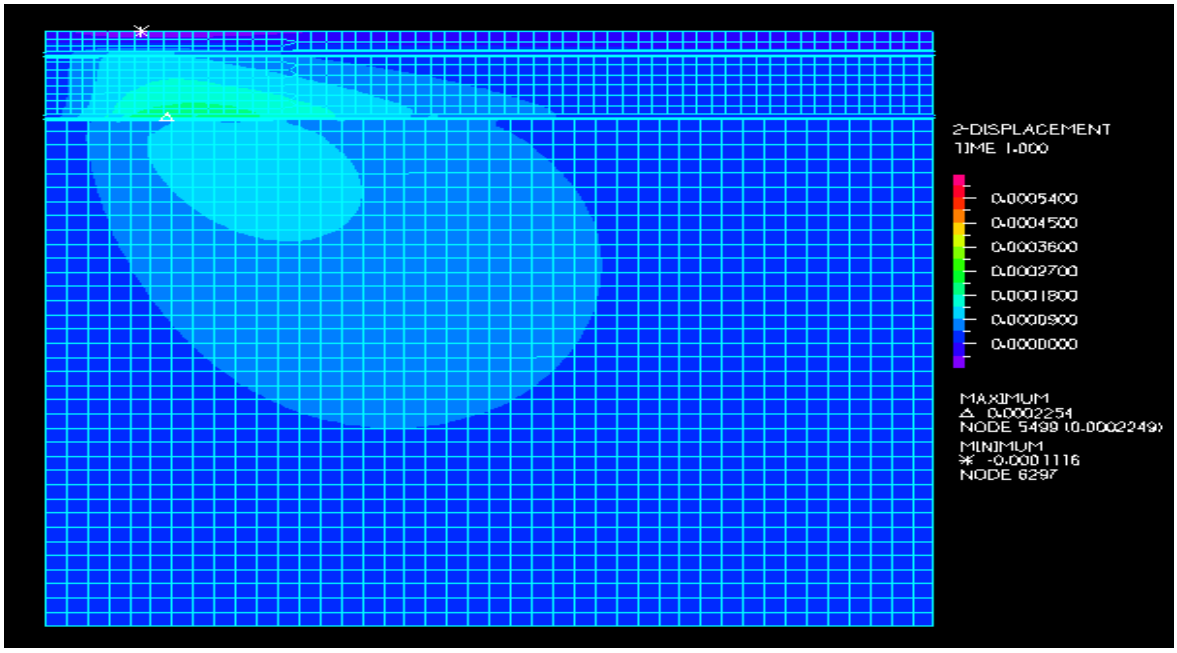

Fig. 4.24: The distribution of horizontal displacement along the pavement cross-section for case of an unreinforced pavement having weak base and silty sand subgrade layer

Figs. 4.25 and 4.26 show the distribution of horizontal displacement along the pavement cross-section for case of a reinforced pavement system having *weak base layer and silty sand subgrade layer* for various values of interface friction.

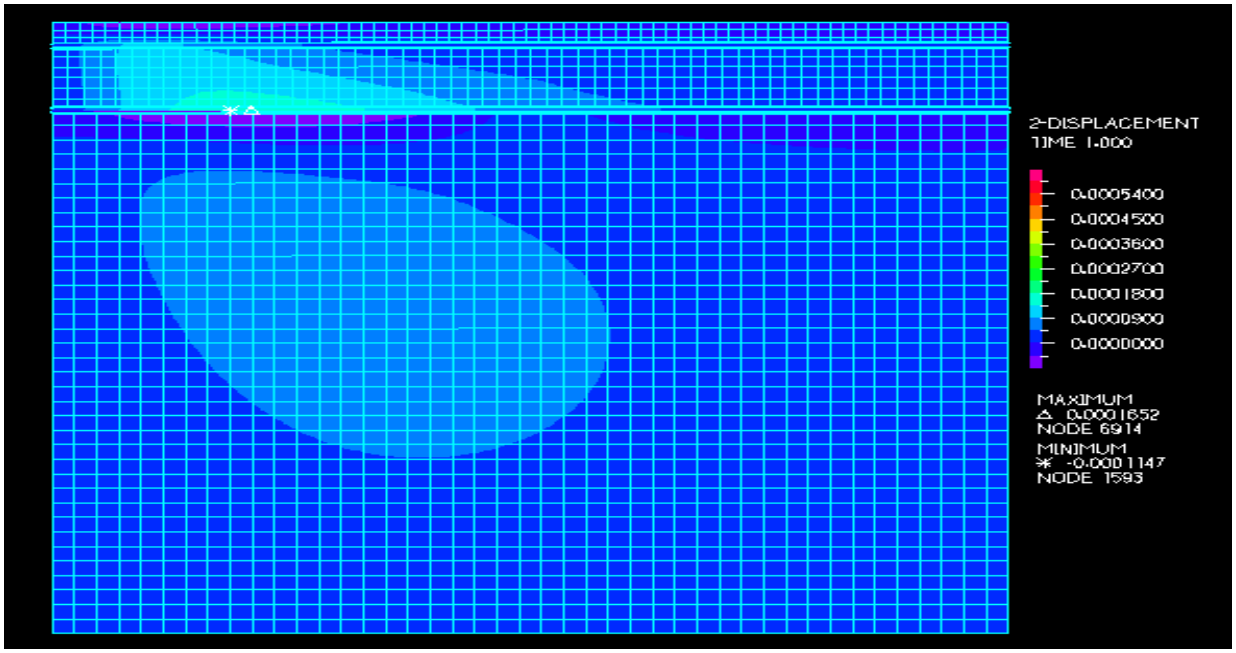

Fig. 4.25: The distribution of horizontal displacement along the pavement cross-section for case of a reinforced pavement μ_1=0; and μ_2=0 havingweak base and silty sand subgrade layer

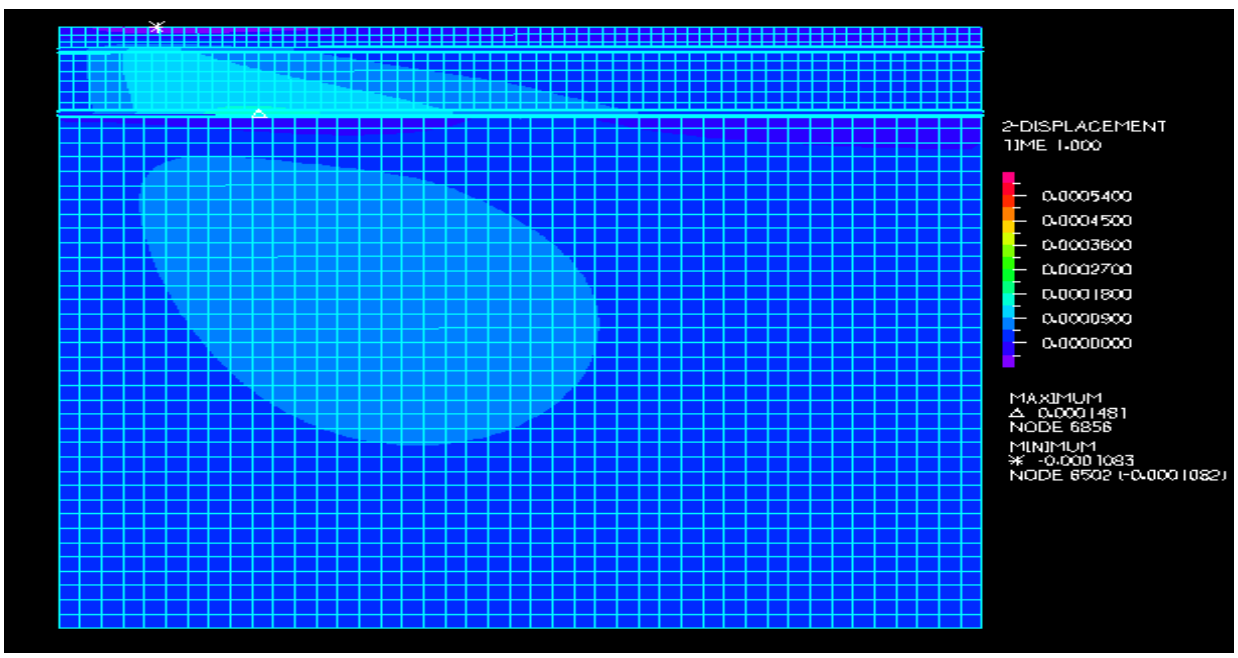

Fig. 4.26: The distribution of horizontal displacement along the pavement cross-section for case of a reinforced pavement μ_1=0.92; and μ_2=0.96 having weak base and silty sand subgrade layer

Fig. 4.27 shows the distribution of horizontal displacement along the pavement cross-section for the case of an unreinforced pavement system having *strong base layer and silty subgrade layer*.

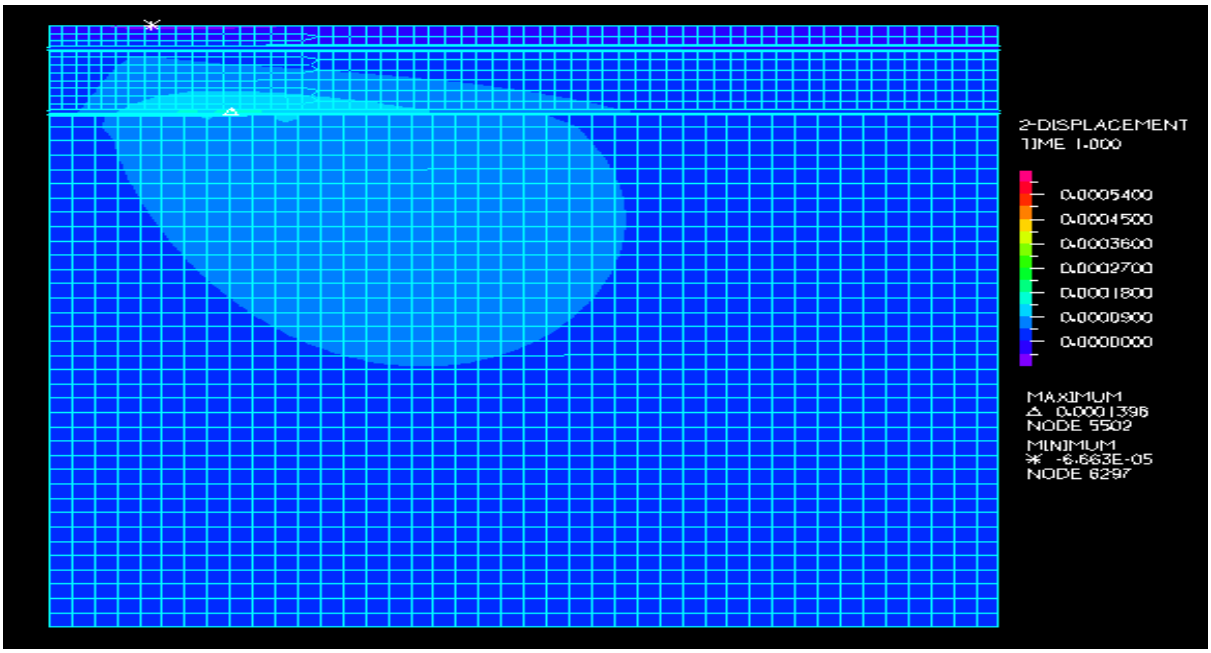

Fig. 4.27: The distribution of horizontal displacement along the pavement cross-section for case of an unreinforced pavement having strong base and silty sand subgrade layer

Figs. 4.28 and 4.29 show the distribution of horizontal displacement along the pavement cross-section for case of a reinforced pavement system having *strong base layer and silty sand subgrade layer* for various values of interface friction.

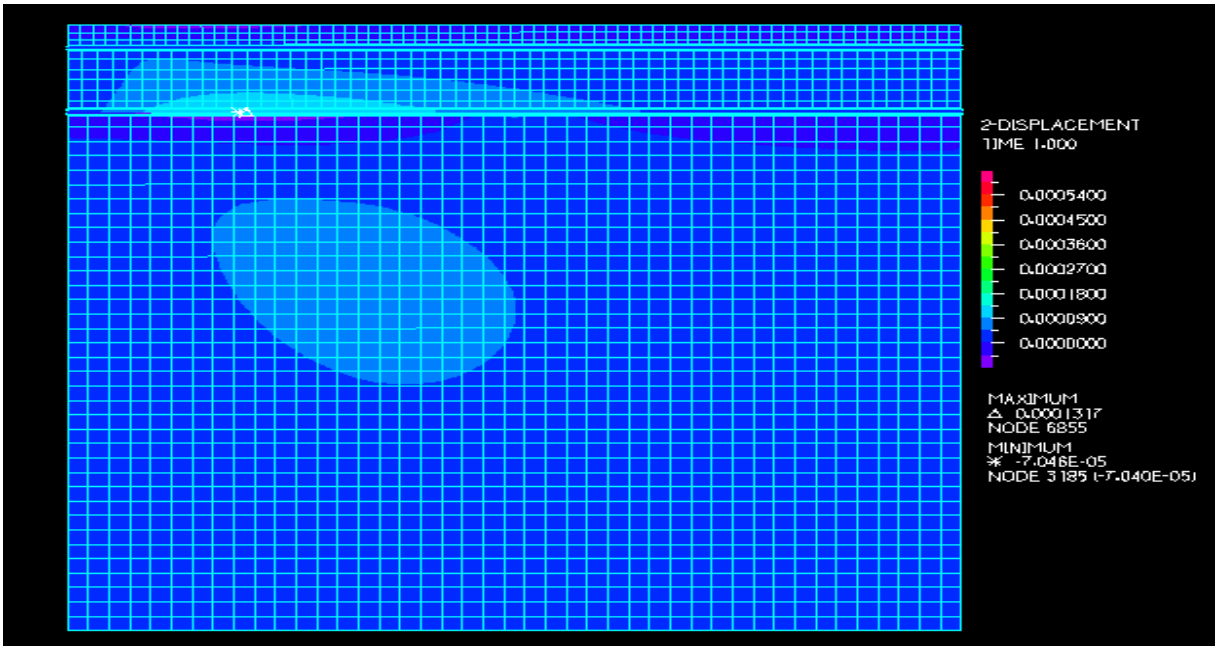

Fig. 4.28: The distribution of horizontal displacement along the pavement cross-section for case of a reinforced pavement μ_1=0; and μ_2=0 having strong base and silty sand subgrade layer

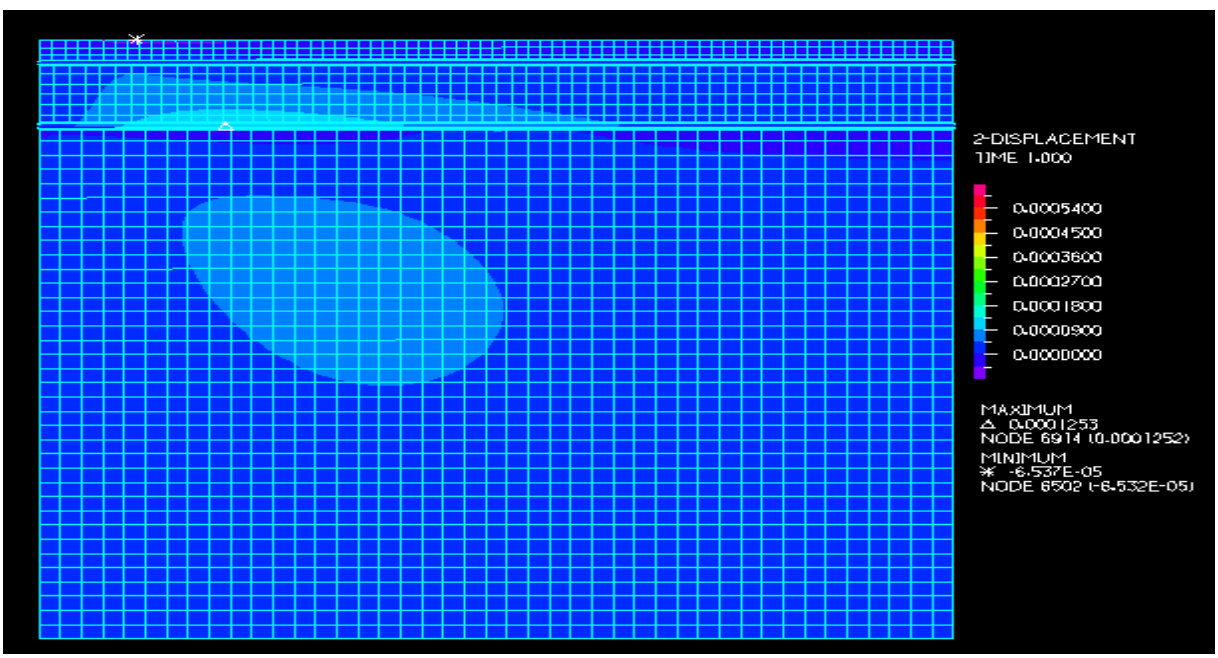

Fig. 4.29: The distribution of horizontal displacement along the pavement cross-section for case of a reinforced pavement μ_1=0.92; and μ_2=0.96 having strong base and silty sand subgrade layer

It can be concluded from observations of Figs 4.16 to 4.29, that the maximum reduction in the horizontal displacement occurs when the friction coefficients equal μ_1= 0.92; μ_2 = 0.96 between the geosynthetic and the foundation layer, and between the geosynthetic and the subgrade respectively. The influence of the geosynthetic is found to decrease when the strength of base layer increases.

4.4 Variation of Vertical Surface Deflection

From the variations of the vertical deflection of the surface (1-2) (Figs. 4.2 to 4.15), the maximum deflections were determined for the various cases and are reported in Table (4.1). The variation of the maximum vertical surface deflection along surface (1-2) (Fig. 4.1) is shown in Figs. 4.30, 4.31, 4.32, and 4.33. It is seen from these figures that the highest reduction of vertical surface deflection in the pavement with weak base layer and weak subgrade layer is about 17% (Table 4.1). This reduction is reached in the case of full bonding between the geosynthetic and the granular base, and between the geosynthetic and the subgrade. In addition, Table (4.1) shows that when the friction coefficient μ between the geosynthetic and the granular base, and between the geosynthetic and subgrade increases the amount of reduction of the vertical surface deflection increases up to 14.54% for μ_1= 0.92 for contact surface between the geosynthetic and the foundation layer; and μ_2= 0.96 for contact between the geosynthetic and cohesive soil. Fig (4.30) shows the amount of reduction in vertical surface deflection for different interface friction values for pavement system of weak base layer and weak subgrade layer.

	Max surface deflection (mm)							
	Weak SG & Weak GB	EFF%	Weak SG & Strong GB	EFF%	Strong SG & Weak GB	EFF%	Strong SG & Strong GB	EFF%
Unreinforced soil	4.249	0.00	2.600	0.00	1.686	0.00	1.036	0.00
Reinforced; μ1=0, μ2=0	3.700	12.92	2.422	6.85	1.688	-0.12	1.049	-1.25
μ1=0.392, μ2=0.294	3.668	13.67	2.411	7.27	1.674	0.71	1.043	-0.68
μ1=0.82, μ2=0.64	3.645	14.22	2.402	7.62	1.662	1.42	1.037	-0.10
μ1=0.92, μ2=0.96	3.631	14.54	2.397	7.81	1.653	1.96	1.032	0.39
Reinforced; Full Bonding	3.542	16.64	2.357	9.35	1.549	8.13	0.96	7.34

Table (4.1): Maximum vertical surface deflection (mm)

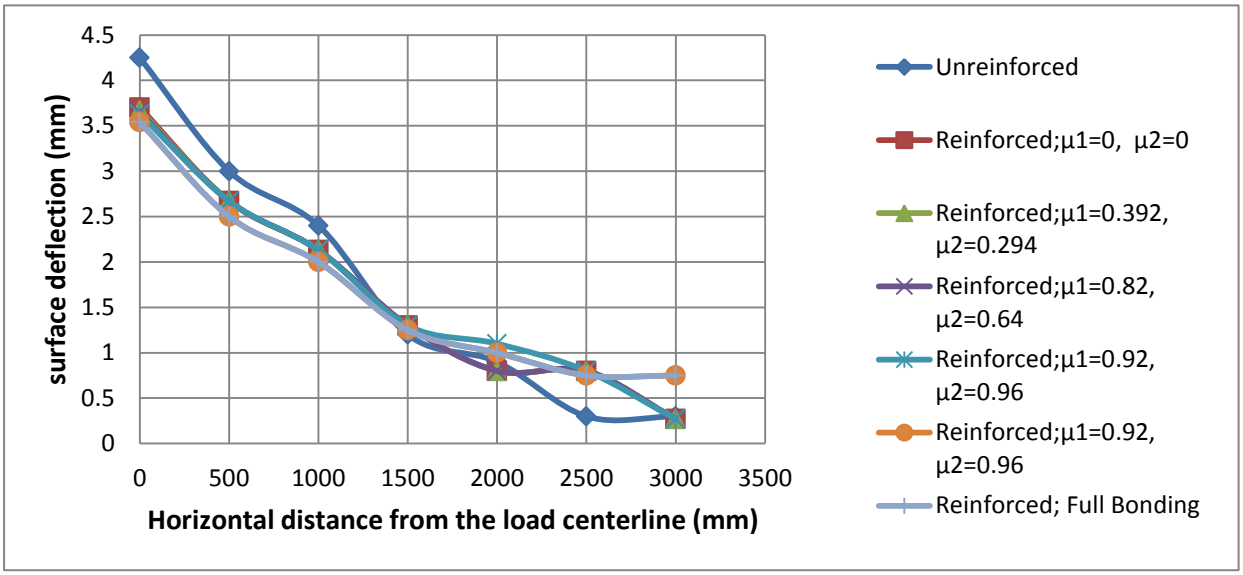

Fig. 4.30: The vertical surface deflection along edge (1-2) for pavement system having weak base layer and weak subgrade layer

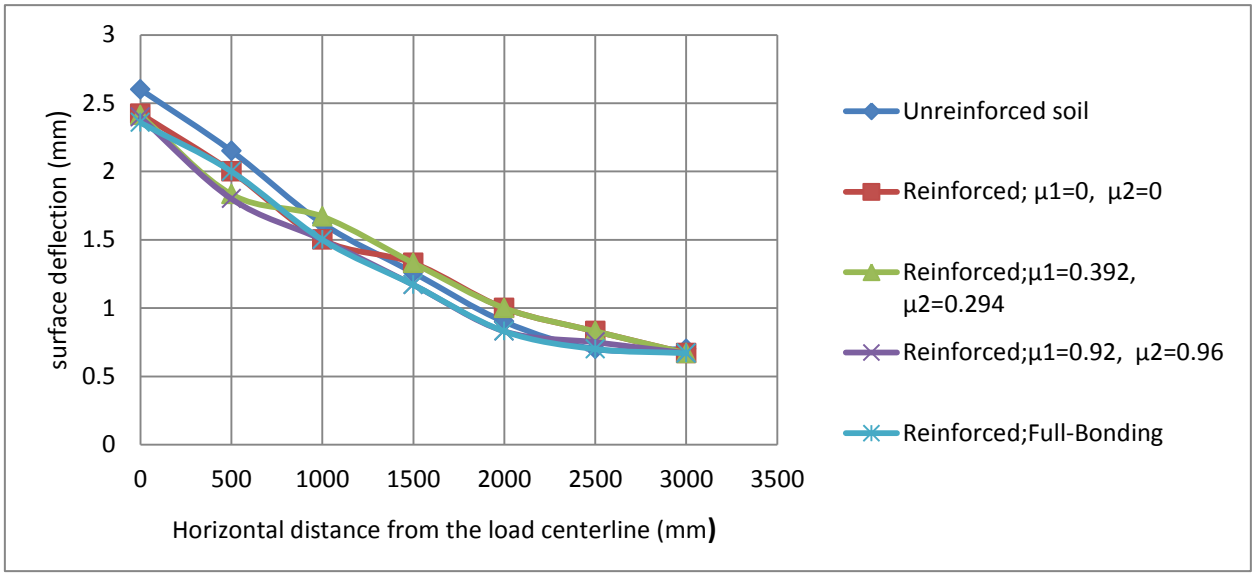

Fig. 4.31: The vertical surface deflection along edge (1-2) for pavement system having strong base layer and weak subgrade layer

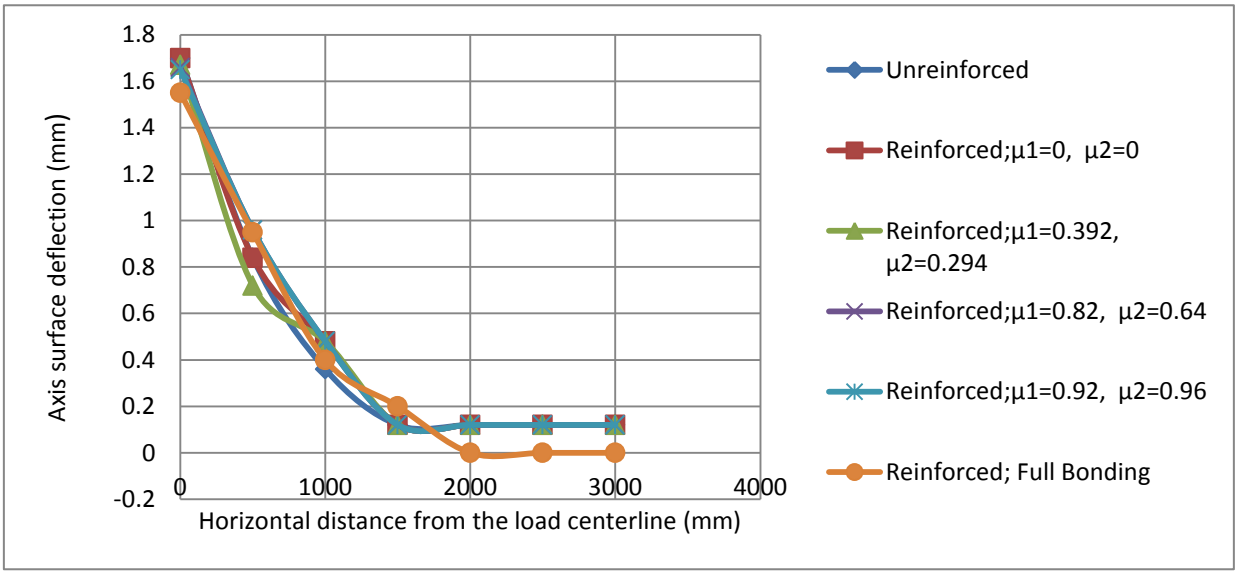

Fig. 4.32: The vertical surface deflection along edge (1-2) for pavement system having weak base layer and silty sand subgrade layer

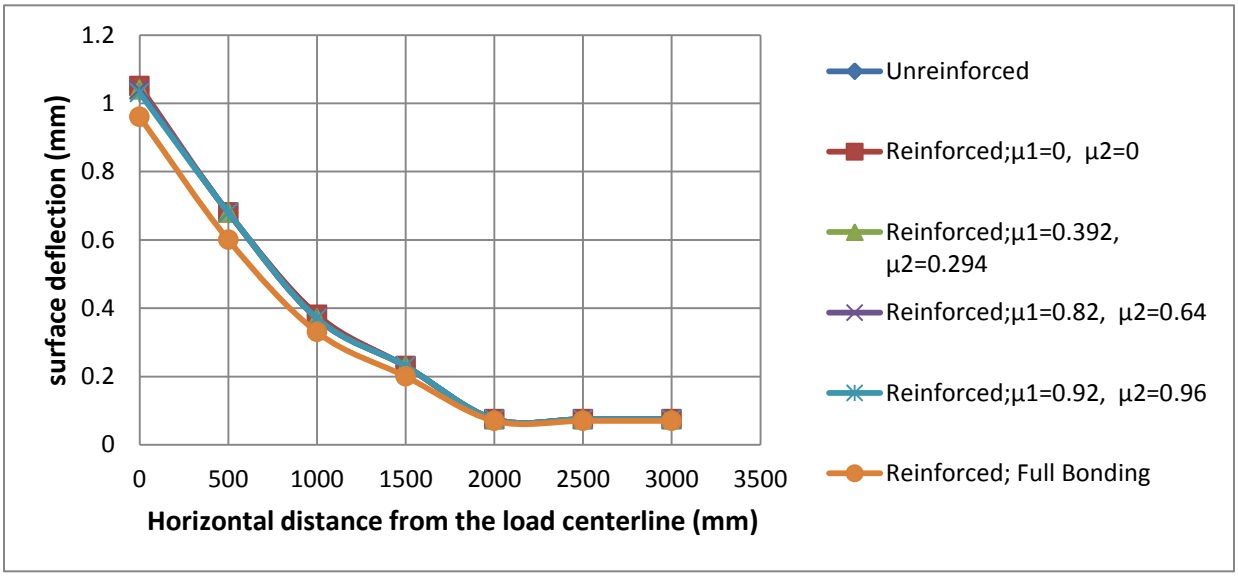

Fig. 4.33: The vertical surface deflection along edge (1-2) for pavement system having strong base layer and silty sand subgrade layer

It is seen from results reported for the pavement of strong foundation layer and weak subgrade layer that the amount of vertical surface deflection is 2.6 (mm) for unreinforced pavement. This amount is decreased when the geosynthetics is placed between foundation layer and subgrade with the highest reduction reaching 9.4% in the case of full bonding at the contact surfaces between the geosynthetic and other pavement layers (granular base, subgrade). In addition, when the friction coefficients of contact surfaces between the geosynthetics and the foundation layer, and between the geosynthetic and the cohesive soil increase, the amount of reduction increases to 7.8% for μ_1= 0.92 at the contact surface between the geosynthetic and the foundation layer; and μ_2= 0.96 for contact surface between the geosynthetic and the cohesive soil.

On the other hand, the influence of interface friction coefficients at the contact surfaces between geosynthetics and the pavement layers (base, and subgrade) on pavement performance decreases for the pavement of weak foundation layer and strong subgrade layer, with the highest reduction reaching only 2%. This amount decreases to 0.4% in the pavement with strong foundation layer and strong subgrade for μ_1= 0.92 at the contact surface between the geosynthetic and the foundation layer; and μ_2= 0.96 for contact surface between the geosynthetic and the cohesive soil.

It can be concluded from these observations that the highest reduction of the vertical surface deflection occurs when the friction coefficients equal μ_1= 0.92; μ_2 = 0.96 between the geosynthetic and the foundation layer, and between the geosynthetic and the subgrade respectively. Additionally, the influence of the geosynthetic is found to decrease when the strength of subgrade layer increases.

4.5 Variation of Horizontal Displacement

The maximum horizontal displacement along the interface between geosynthetic and pavement layers is reported in Table (4.2) for the various sections analyzed. The variation of the maximum horizontal displacement along the interface between geosynthetics and pavement layers is shown in Figs. 4.34, 4.35, 4.36, and 4.37. Table (4.2) shows that the highest reduction of horizontal displacement in the pavement of weak base layer and weak subgrade layer is 49.74%. This reduction is reached in the case of full bonding between the geosynthetic and the granular base layer, and between the geosynthetic and the subgrade layer. In addition, (Table 4.2) shows that when the friction coefficients μ between the geosynthetic and the granular base and between the geosynthetic and subgrade increase, the amount of reduction of the horizontal displacement increases until it reaches 46.4 % for μ_1= 0.92 at the contact surface between the geosynthetic and the foundation layer and μ_2= 0.96 for contact surface between the geosynthetic and cohesive soil layer. The distribution of maximum horizontal displacement along the contact surfaces between the geosynthetic layer and the pavement layers (base and subgrade layers) is shown in Fig.4.34 for the pavement system having weak base layer and weak subgrade layer.

	Horizontal displacement (mm)							
	Weak SG & Weak GB	EFF%	Weak SG, Strong GB	EFF%	Strong SG & Weak GB	EFF%	Strong SG & Strong GB	EFF%
Unreinforced soil	0.567	0.00	0.265	0.00	0.225	0.00	0.140	0.00
Reinforced; μ1=0, μ2=0	0.323	43.03	0.214	19.25	0.165	26.67	0.132	5.71
μ1=0.392, μ2=0.294	0.315	44.44	0.211	20.38	0.16	28.89	0.129	7.86
μ1=0.82, μ2=0.64	0.308	45.68	0.209	21.13	0.153	32.00	0.127	9.29
μ1=0.92, μ2=0.96	0.304	46.38	0.207	21.89	0.148	34.22	0.125	10.71
Reinforced; Full Bonding	0.285	49.74	0.197	25.66	0.11	51.11	0.103	26.43

Table (4.2): Maximum horizontal displacement (mm)

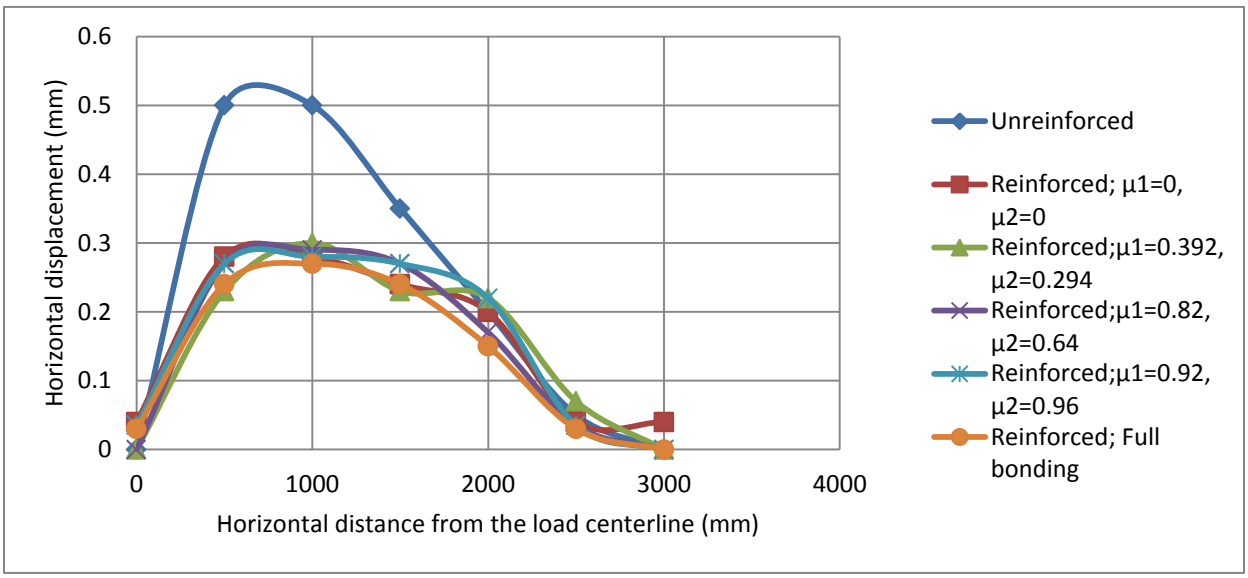

Fig. 4.34: The horizontal displacement along edge (3-4) for pavement system having weak base layer and clayey subgrade layer

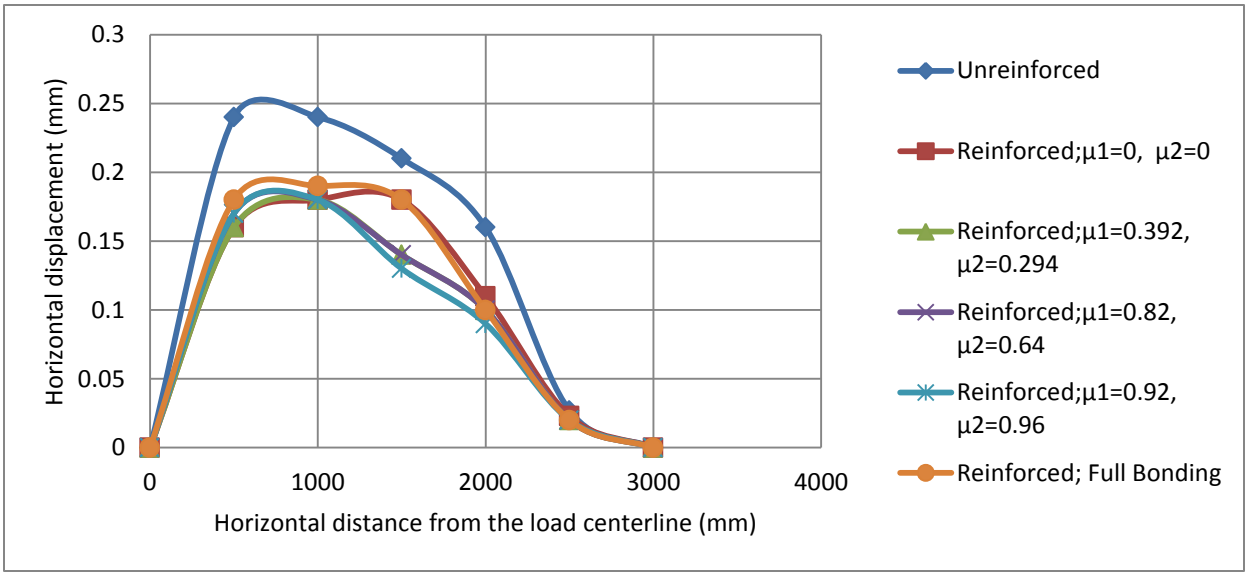

Fig. 4.35: The horizontal displacement along edge (3-4) for pavement system having strong base layer and clayey subgrade layer

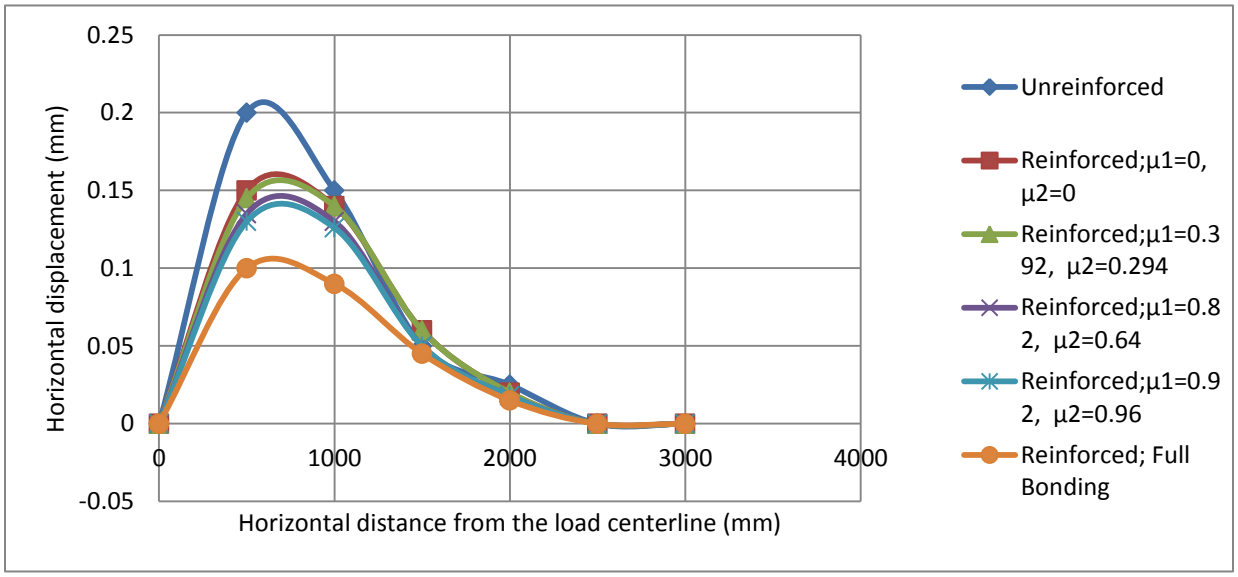

Fig. 4.36: The horizontal displacement along edge (3-4) for pavement system having weak base layer and silty sand subgrade layer

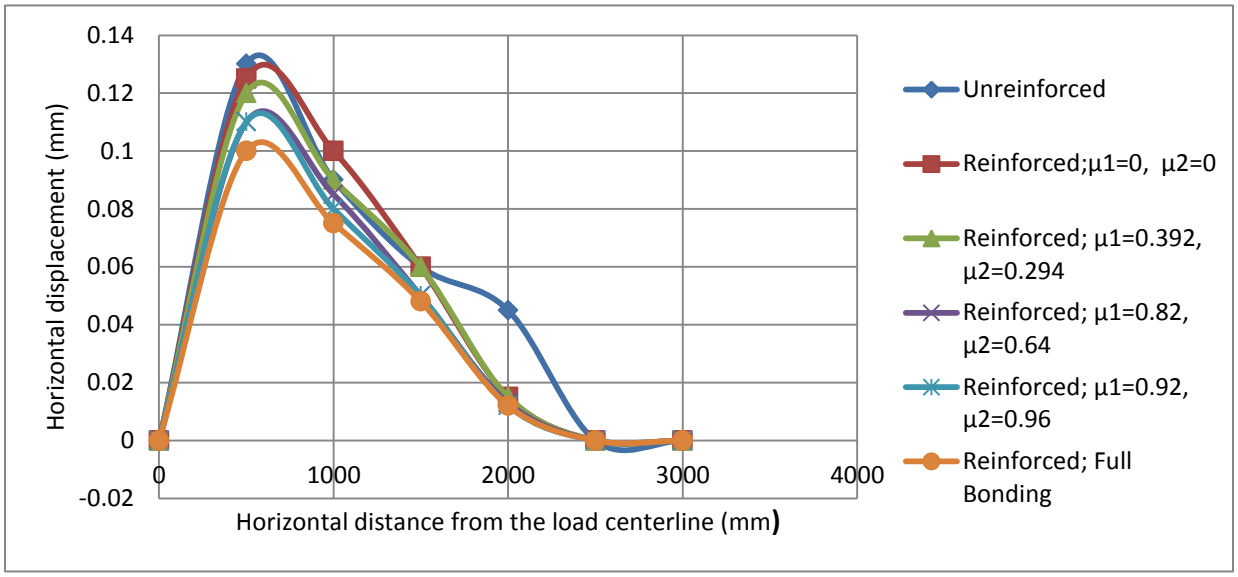

Fig. 4.37: The horizontal displacement along edge (3-4) for pavement system having strong base layer and silty sand subgrade layer

It is also observed that for the pavement of strong foundation layer and weak subgrade layer that the amount of horizontal displacement decreases when the geosynthetic is placed between the base and subgrade layers. The amount of decrease is dependent on the amount of friction coefficients between the geosynthetic layer and the pavement layers (base and subgrade). For example, when $\mu = 0$ between two contact surfaces of geosynthetics and pavement layers (base and subgrade) the amount of horizontal displacement reached 0.214 (mm), while it reaches 0.207 (mm) when $\mu_1 = 0.92$, and $\mu_2 = 0.96$; between the geosynthetic and the foundation layer, and between the geosynthetic and subgrade respectively as shown in Table (4.2).

On the other hand, the influence of geosynthetic on the pavement performance increases for pavements with weak foundation layer and strong subgrade layer, with the highest reduction reaching 51.1% .This reduction is reached for the case of full bonding between the geosynthetic and the granular base layer, and between the geosynthetic and the subgrade layer. In addition, Table (4.2) shows that when the friction coefficient μ between the geosynthetics and the granular base and between the geosynthetics and subgrade increases the amount of horizontal displacement reduction increases to 34.2% for $\mu_1 = 0.92$ at the contact surface between the geosynthetic and the foundation layer; and $\mu_2 = 0.96$ for contact surface between the geosynthetic and cohesive soil Fig (4.34). In contrast, the amount of reduction of the horizontal displacement decreases for the pavement of strong foundation layer and strong subgrade layer to 0.125 (mm) for $\mu_1 = 0.92$; $\mu_2 = 0.96$, while reaches 0.14 (mm) for unreinforced pavement Fig. 4.35. These observations show that the maximum horizontal displacement occurs at the contact surface between foundation layer and cohesive soil layer in the unreinforced pavement and the geosynthetic reinforced pavement.

In addition, the maximum reduction in the horizontal displacement occurs when the friction coefficients equal μ_1= 0.92; μ_2 = 0.96 between the geosynthetic and the foundation layer, and between the geosynthetic and the subgrade respectively. Also, the influence interface friction coefficients at the contact surfaces between the geosynthetics and the pavement layers decreases when the strength of base layer increases.

4.6 Comparison of Results

The results obtained in this study are compared with the results of past studies. The comparison shows that good agreement is obtained concerning the following observations: 1) the strength of subgrade has a significant effect on the performance of the reinforcement pavement. The influence of geosynthetics as a reinforcement material is beneficial for weak subgrade foundation (Nazzal et al. 2006, Wathugala et al. 1996 and Saad et al. 2006); 2) the reduction of vertical surface deflection is also dependent on the strength of subgrade layer and the strength of foundation layer, geosynthetic stiffness, and the thickness of the foundation layer Nazzal et al. (2006). In this study, the effect of subgrade stiffness and the foundation layer stiffness have been investigated. It was found that the reduction of vertical surface deflection reaches to (16%), this is close to the other studies' results, refer to Saad et al. (2006), Wathugala et al. (1996), and Dondi (1994) which found the reduction of vertical surface deflection will be in range (14% - 34%).

CHAPTER FIVE

CONCLUSIONS AND RECOMMENDATIONS

5.1 Conclusions

A series of finite element simulations were conducted to investigate the benefits of using geosynthetics in pavement sub layers for different cases of base course and subgrade; weak versus strong. The results of these simulations have provided insights into the effects of the interface friction coefficient between geosynthetic and base courses on vertical surface deflection and horizontal displacement of layers, as summarized below:

1) The highest reduction of the vertical surface deflection is observed for pavement with weak base and weak subgrade layer. This reduction, which reaches nearly 14.5% is achieved when the friction coefficients of the interface reach to $\mu_1 = 0.92$ and $\mu_2 = 0.96$, respectively. Note that these values were recommended by Koerner (1994). In addition, the amount of reduction on the vertical surface deflection for a reinforced pavement structure is found to decrease when the strength of subgrade increases to reach 2% for the pavement system having strong subgrade and weak granular base.
2) The strength of the base layer has a significant effect on horizontal displacement. The highest reduction of the horizontal displacement is reached for the pavement with weak granular base and weak subgrade. This reduction, which reaches 46%, is achieved when the friction coefficients of the interface reach to $\mu_1 = 0.92$ and $\mu_2 = 0.96$, respectively. Such influence is found to reduce when the stiffness of the granular base increased.

It is evident from these studies that the interface friction between the geosynthetics and the pavement layers (base and subgrade) affected the performance of the pavement structure the most. The best results can be achieved when the friction coefficients of the interface equal $\mu_1 = 0.92$ and $\mu_2 = 0.96$, confirming the observations made by Koerner (1994).

5.2 Recommendations

The numerical analyses here were conducted to study the performance of reinforced and unreinforced pavement cross-section under monotonic loadings. It is recommended to extend the study to cyclic loadings. While the effects of interface friction between the geosynthetic and soil layers on reinforced pavement performance is highlighted by this study using parametric studies, it would be of use to quantify the actual values in the future for the various geosynthetics and soils. It is also recommended to use the concept of interface interlocking and shear strength towards the purpose.

References

Adina R&D Inc. (Adina R&D). (2001). “Finite element computer program, theory and modeling guide.” Rep. ARD 01-7, Vol. 1, Adina R&D Inc., Watertown, Mass.

Barksdale, R. D., Brown, S. F., and Chan, F., (1989). "Potential benefits of geosynthetics in flexible pavement systems." *National cooperative highway research report No.315,* TRB national Research Council, Washington, DC, 1-53.

BOSTD Geosynthetics., (2007). “Soil-geogrid friction coefficients.” *pp* 2.1-2.5 http://www.newgrids.com/userImages/00000126_Design%20Factors%20Section%202%20Friction.pdf

Brocklehurst, J.C., (1993). “Finite element studies of reinforced and unreinforced two-layer soil system.” *A Thesis Ssubmitted for the Degree of Doctor of Philosophy at the University of Oxford.*

Brown, S.F., Brunton, J.M., Hughes, D.A.B., and Brodrick, B.V., (1985). “Polymer grid reinforcement of asphalt.” *Proc., Assoc. of Asphalt Paving Technologists,* 54, 18-41.

Chen, W, F., and Baladi, G, Y., (1985). “Soil plasticity; Theory and implementation.” *Elsevier Science*

Cho, Y., McCullough, B. F., and Weissmann, J., (2000). "Consideration on finite-element method application in pavement structural analysis." *Transportation Research Record 1539,* TRB national Research Council, Washington, DC , 96-101.

Collins, I, F., (2005). “The concept of stored plastic work or frozen elastic energy in soil mechanics.” *Geotechnique,* 55. 373-382

Davies, M.C.R. and Bridle, R.J., 1990, “Predicting the Permanent Deformation of Reinforced Flexible Pavement Subject to Repeated Loading.” *Performance of Reinforced Soil Structures*, 421-425.

Desai, C, S., and Siriwardane, H, A., (1984). "Constitutive laws for engineering material." *Prentice-Hall,Englewood cliffs, N. J.*

Desai, C, S., Somasundaram, S., Frantziskonis, G, N., and Hierarchical, A., (1986). "Approach for constitutive modeling of Geologic materials." *International Journal for Numerical and Analytical Methods in Geomechanics,* 10. 225-257

Diambra, A., Ibraim, E., Muir Wood, D., and Russell, A, R., (2010). "Fibre reinforced sands: Experiments and modeling." *Geotextiles and geomembranes,* 28, 238-250.

Dondi, G., (1994). “Three-dimensional finite element analysis of a reinforced paved road." *Fifth international conference on geotextiles, geomembranes and related products Singapore*, 1, 95-100.

Haas, R., Walls, J., and Carroll, R.G., (1988). "Geogrid reinforcement of granular bases in flexible pavements." *Transportation Research Record 1188*, 19-27.

Hausmann, M, R., (1990). “Engineering principles of ground modification.” *McGraw-Hill.*

Holtz, R, D., Christopher, B, R., and Berg, R, R., (1998). "Geosynthetic design and construction guidelines." *Federal highway administration, Washington DC, FHWA/HI-98/038. 460p*

Howard, I., and Warren, K., (2006). "Finite element approach for flexible pavements with geosynthetics." *GeoCongress 2006-ASCE*. 187-192

Juran, I., Guermazi, A., Chen, C.L., and Ider, M.H., (1988). "Modelling and simulation of load transfer in reinforced soils: part 1." *International Journal for Numerical and Analytical Methods in Geomechanics*, 12, 141-155.

Juran, I., Ider, M, H., Chen, C.L., and Guermazi, A., (1988). "Numerical analysis of the response of reinforced soils to direct shearing: Part 2." *International Journal for Numerical and Analytical Methods in Geomechanics*, 12, 157-171.

Koerner, R, M., (1994). “Designing with geosynthetics; Third edition.” *Prentice-Hall, Inc.*

Ling, H, I., and Liu, K., (2003). "Finite element studies of asphalt concrete pavement reinforced with *geogrid* ." *Engineering mechanics-ASCE*, 129. 801-811

Ling, H, I., and Liu, Z., (2001). "Performance of geosynthetic-reinforced asphalt pavements." *Geotechnical and geoenviromental engineering*. 177-184

Nazzal, M, D., Abu-Farsakh, M, Y., and Mohammad, L, N., (2006). "Numerical analysis of geogrid reinforcement of flexible pavements." *GeoCongress 2006-ASCE. 1-6*

Penner, R., Haas, R., Walls, J., and Kennepohi, G., (1985). "Geogrid reinforcement of granular bases." Paper presented at the *Transportation Association of Canada Annual Conference*, Vancouver, British Columbia, Canda.

Perkins, S.W., (1999). “Mechanical response of geosynthetic-reinforced flexible pavements: Technical paper.” *Geosynthetics international*, 6. 347-381

Perkins, S.W., (2001). “Numerical modeling of geosynthetic reinforced flexible pavement: Final report.” *Rep. No. FHWA/MT-01/003/99160-2*, Montana Department of Transportation, Helena, Mont.

Perkins, S.W., and Ismeik, M., (1997). “A synthesis and evaluation of geosynthetic-reinforced base layers in flexible pavements: part 2.” *Geosynthetics International*. 4, 605-621.

Rowe, R, K., and Skinner, D, G., (2001). "Numerical analysis of geosynthetic reinforced retaining wall constructed on a layered soil foundation." *Geotextiles and geomembranes* , 19. 387-412

Saad, B., Mitri, H., and Poorooshasb, H., (2006). "3D FE analysis of flexible pavement with geosynthetic reinforcement." *J. Transportation Engineering 132,* 402-415.

Wang, J., Dove, J, E., and Gutierrez, M, S., (2007). "Anisotropy-base failure criterion for interface systems." *Geotechnical and geoenviromental engineering*, 133. 599-608

Wathugala, G, W., and Desai, C, S., (1993). "Constitutive model for cyclic behavior of clay I: Theory." *Geotechnical engineering,* 119. 714-729

Wathugala, G.W., Huang, B., and Pal, S., (1996). "Numerical simulation of geosynthetic reinforced flexible pavement." *Transportation Research Record 1534,* TRB national Research Council, Washington, DC , 12, 58-65.

Yan, Q., Mei, Y., Li, C., and Deng, W., (2010). "Study on the characteristics of geogrids / soil interface." *Mechanic Automation and Control Engineering (MACE), 2010 International Conference,* 1241 - 1248.

Zornberg, J.G. (2011). “Advances in the use of geosynthetics in pavement design." *Geosynthetics India,* 11, 3-21.